THIRTEEN-COLOR PHOTOMETRY OF SUBDWARF STARS. I
OBSERVATIONS, SENSITIVITY OF THE INDICES, AND EVOLUTIONARY EFFECTS

WILLIAM J. SCHUSTER

Instituto de Astronomía
Universidad Nacional Autónoma de México

RESUMEN

Se presentan observaciones de 118 estrellas subenanas y de algunas estrellas de las Hyadas en el sistema fotométrico de 13 colores de ancho de banda intermedia-angosta. Se compara la fotometría de las subenanas con los colores promedio de las Hyadas a temperatura efectiva constante para construir curvas de encubrimiento. En forma similar hemos comparado gigantes y subgigantes para derivar curvas de gravedad. Para las temperaturas correspondientes a estrellas tipo F, G o K-tempranas en la secuencia principal, los índices de 13 colores separan claramente los efectos de temperatura, metalicidad y gravedad superficial. Los colores $45 - 63$ y $58 - 99$ sirven para medir la temperatura, $37 - 45$ es muy sensitivo a la metalicidad y $G = (35 - 52) - (37 - 45)$ es un buen índice de gravedad.

Se hace una analogía clara entre las posiciones de las subenanas en el diagrama (G, $45 - 63$) y los diagramas color-magnitud de los cúmulos globulares. Las subenanas muestran una secuencia principal no evolucionada para $45 - 63 > 0.75$, una secuencia principal evolucionada para $45 - 63 < 0.75$, un punto de partida en $45 - 63 \sim 0.59$, y una rama subgigante-gigante. Estos resultados corroboraron independientemente las conclusiones de Cayrel (1968), Sears y Whitford (1969), y Eggen (1973).

Sin embargo, algunas subenanas evolucionadas son considerablemente más rojas que el punto de partida de nuestro cúmulo hipotético pero no caen cerca de la envoltura subgigante-gigante. No se pueden explicar los colores de estas subenanas por enrojecimiento interestelar, por contaminación de la fotometría, ni por encubrimiento residual en el índice G. Estas subenanas frías y evolucionadas indican que los objetos de Población II extrema se formaron durante un período por lo menos de 2×10^9 años. Se discuten las implicaciones cosmológicas de tal diferencia de edades de las subenanas.

ABSTRACT

The 13-color medium-narrow-band photometric system has been used to observe 118 subdwarfs and a number of Hyades stars. The subdwarf photometry has been compared to mean Hyades colors at constant effective temperature in order to construct blanketing curves. By a similar process giants and subgiants have been used to derive gravity-difference curves. For the temperature range of F, G, and early-K main sequence stars the 13-color indices give a clear separation between the effects of temperature, metallicity, and surface gravity: $45 - 63$ and $58 - 99$ are good for measuring temperature, $37 - 45$ is very sensitive to metallicity, and $G = (35 - 52) - (37 - 45)$ is a good gravity index.

A clear analogy between the positions of the subdwarfs in the (G, $45 - 63$) diagram and globular cluster color-magnitude diagrams has been drawn. The subdwarfs show an unevolved main sequence for $45 - 63 > 0.75$, an evolving main sequence for $45 - 63 < 0.75$, a turnoff at $45 - 63 \sim 0.59$, and a subgiant-giant branch. These results represent a completely independent corroboration of the conclusions made by Cayrel (1968), Sears and Whitford (1969), and Eggen (1973).

However, a number of evolved subdwarfs are significantly redder than the turnoff of our hypothetical cluster but do not lie near the subgiant-giant envelope. The colors of these subdwarfs can not be explained by interstellar reddening, nor by contamination of the photometry, nor by a residual blanketing in the G index. These cooler evolving subdwarfs indicate that the extreme Population II objects formed over a time interval of at least 2×10^9 years. The cosmological implications of such a range in subdwarf ages are discussed.

233

I. INTRODUCTION

The thirteen-color medium-narrow-band photometric system was originally designed for the study of early-type stars (Johnson, Mitchell and Latham 1967) with the seven bluest filter bands matching closely those chosen by Borgman (1960) for the study of O, B, and A stars. However, Borgman's (1962) own work, as well as the results of Smith (1968), Mitchell and Johnson (1969), and Schuster (1976a), has shown that these photometric systems can also provide very useful data concerning later-type stars, such as F and G-type subdwarfs and solar type stars.

The present work was motivated by the photometric, multi-band studies of the spectral-energy distribution of subdwarfs by Johnson, MacArthur and Mitchell (1968) and by Johnson and Mitchell (1968). These works studied the difference in the spectral-energy curves between subdwarfs and Hyades main sequence stars of equal effective temperature assuming that the temperature index $R - I$ is independent of the stellar atmospheric metal content. Their results were presented in the form of blanketing curves such as Figure 7 of Johnson et al. (1968) and Figure 2 of Johnson and Mitchell (1968). In this paper we will study the temperature, metallicity and surface gravity sensitivities of the 13-color indices by deriving blanketing and gravity-difference curves. We will make use of the $45 - 63$ temperature index as suggested by Johnson and Mitchell (1968), and metallicity and gravity corrections for this index will come from theoretical 13-color photometry derived from the model atmosphere work of Kurucz (1975). In later papers we will calibrate the appropriate indices, as found in this paper, for temperature, composition and surface gravity and then use these calibrations to study the subdwarfs.

II. THE OBSERVATIONS

The 13-color medium-narrow-band photometric system has been defined by the articles and observations of Johnson et al. (1967), Mitchell and Johnson (1969), and Johnson and Mitchell (1975). This system is made up of two parts — an 8 color (8C) part using filters with effective wavelengths from 3370Å to 6350Å and a 6 color (6RC) part

using filters from 5830Å to 1.1μ. The names which are used for the filters are obtained from their effective wavelengths; the filter band with an approximate effective wavelength of 0.33μ produces the 33 magnitude, and so forth. The most recent absolute energy calibration for the entire 13-color system has been published by Johnson and Mitchell (1975).

The 118 subdwarfs observed in our program were selected primarily from Eggen's (1964) list of high velocity objects with a few others being added from the works of Roman (1955), Eggen and Sandage (1959, 1962), Sandage and Eggen (1959), Sandage and Smith (1963), Strom and Strom (1967), Johnson et al. (1969) and Gliese (1969). The 13-color observations of the subdwarfs and of Hyades stars, given in Tables 1 and 2 respectively, were carried out during 1973 and 1974 using the 152 cm. (60″) and 84 cm (33″) telescopes of San Pedro Mártir Observatory in Baja California (hereinafter referred to as 'SPM') with only a few 8C observations coming from Johnson and Mitchell (1968). In Table 2 about 40% of the 8C photometry comes from 'SPM' and about 60% of the 6RC data; the rest comes from other sources (Johnson and Mitchell 1968; Mitchell and Johnson 1969). We encountered no problems in transforming our subdwarf and Hyades observations onto the standard 13-color system since we observed with the original filters and photomultipliers used to define this system.

In Table 1 column 1 gives the subdwarf name, column 2 gives the 52 magnitude, columns 3 to 14 the other 12 filters reduced as colors with respect to the 52 filter, and column 15 the number of blue (8C) and red (6RC) observations NB and NR respectively A. 'D' following the star name in column 1 indicates that the photometry was contaminated by a fainter nearby star which may contribute one percent or more of the light measured. In Table 2 the data are presented as in Table 1 except that columns 10 to 14 give the 6RC colors with respect to filter 58. At the 110 filter the RCA 7102 phototube is about 3 magnitudes less sensitive than for the other 6RC filters, and for this reason many of the subdwarfs were not measured at 1.1μ; and for many that were observed at 1.1μ, problems were encountered. In column 14 of Table 1 a question mark indicates that the value for the 52 −

TABLE 1

13-COLOR PHOTOMETRY OF SUBDWARFS

Name	52	33-52	35-52	37-52	40-52	45-52	52-58	52-63	52-72	52-80	52-86	52-99	52-110	NB/NR
+54°223	5.362	0.484	0.351	0.615	0.788	0.314	0.368	0.606	0.803	1.000	1.051	1.188	1.291	4/4 (4)
- 9°256	9.069	0.340	0.232	0.454	0.664	0.294	0.291	0.492	0.714	0.865	0.925	0.989	1.143	4/4 (2)
+19°279	5.464	0.966	0.862	1.122	1.022	0.332	0.459	0.710	0.945	1.141	1.221	1.337	1.452	9/8 (7)
-16°295	3.690	0.652	0.501	0.753	0.845	0.328	0.380	0.630	0.845	1.026	1.104	1.209	1.342	8/8 (8)
-26°828	6.532	0.595	0.482	0.752	0.836	0.331	0.383	0.621	0.833	1.017	1.081	1.186	1.325	6/7 (7)
-17°484	10.610	-0.023	-0.062	0.097	0.442	0.266	0.239	0.416	0.580	0.729	0.785	0.805	...	4/3 (0)
-13°482	9.902	-0.014	-0.047	0.084	0.422	0.232	0.263	0.398	0.638	0.760	0.821	0.862	...	3/3 (0)
-26°957	8.896	0.350	0.243	0.400	0.646	0.286	0.289	0.488	0.750	0.858	0.927	0.979	1.112	3/4 (4)
G4-37	11.543	0.010	-0.101	0.153	0.467	0.258	0.244	0.441	0.645	0.838	0.902	0.934	...	4/3 (0)
+33°529	10.082	1.976	1.662	1.857	1.618	0.456	0.828	1.271	1.684	2.051	2.197	2.406	2.604	5/3 (3)
-13°544	6.277	1.106	0.957	1.189	1.067	0.341	0.492	0.766	0.982	1.181	1.269	1.386	1.593	4/4 (3)
+25°495	8.185	-0.061	-0.156	0.131	0.477	0.278	0.262	0.455	0.647	0.789	0.852	0.888	1.017	4/4 (3)
G78-26D	11.038	1.577	1.504	1.835	1.495	0.405	0.777	1.215	1.489	1.808	1.960	2.137	...	3/3 (0)
+11°468	10.890	0.092	-0.004	0.248	0.599	0.311	0.290	0.494	0.781	0.918	0.922	1.001	...	4/2 (0)
G5-36	10.908	0.210	0.058	0.261	0.566	0.297	0.264	0.477	0.679	0.829	0.925	0.923	...	4/3 (0)
G38-1	11.588	...	1.717	1.919	1.739	0.491	0.834	1.248	1.756	2.085	2.236	2.466	...	3/4 (0)
- 7°603	8.389	0.360	0.248	0.487	0.688	0.309	0.331	0.551	0.766	0.928	1.022	1.040	1.219	3/3 (2)
- 3°592	6.849	0.231	0.094	0.303	0.601	0.280	0.282	0.488	0.675	0.829	0.882	0.954	0.986	4/4 (2)
+34°796	8.769	1.177	0.674	0.996	1.057	0.421	0.478	0.770	1.066	1.283	1.372	1.501	1.669	4/4 (4)
+21°607	9.329	0.000	-0.095	0.149	0.446	0.249	0.220	0.425	0.594	0.740	0.760	0.777	...	3/4 (0)
G175-39	8.583	1.257	1.115	1.357	1.094	0.334	0.529	0.784	0.981	1.205	1.292	1.419	...	4/4 (0)
+45°992	7.091	0.327	0.197	0.418	0.648	0.290	0.326	0.532	0.729	0.883	0.978	1.023	1.376	4/3 (3)
G102-22	11.820	...	2.404	2.085	1.987	0.834	0.577	1.293	2.501	3.259	3.576	4.064	4.384	4/2 (2)
G99-31D	11.543	0.256	0.151	0.450	0.700	0.298	0.328	0.530	0.826	0.907	1.051	1.117	...	2/2 (0)
+37°1312	7.554	1.008	0.864	1.113	1.008	0.321	0.460	0.727	0.913	1.154	1.195	1.348	1.385	4/4 (4)
+19°1185A	9.450	0.246	0.154	0.422	0.680	0.300	0.353	0.578	0.838	1.059	1.149	1.204	1.255?	4/4 (2)
-0°1520	9.111	0.277	0.191	0.399	0.647	0.285	0.279	0.490	0.699	0.854	0.909	0.993	1.072??	4/4 (4)
+47°1419	5.699	0.325	0.211	0.438	0.651	0.283	0.298	0.502	0.662	0.815	0.870	0.943	1.138	4/4 (4)
-33°4113	5.425	0.218	0.126	0.372	0.670	0.315	0.263	0.464	0.655	0.814	0.922	0.986	1.034	2/4 (4)

TABLE 1 - Continued

Name	52	33-52	35-52	37-52	40-52	45-52	52-58	52-63	52-72	52-80	52-86	52-99	52-110	NB/NR
+31°1684	8.413	0.219	0.049	0.375	0.684	0.330	0.320	0.565	0.809	0.936	1.006	1.108	1.195	4/4 (3)
- 1°1883	7.606	0.543	0.404	0.696	0.827	0.332	0.381	0.635	0.827	1.052	1.175	1.275	1.433	4/4 (3)
+29°1664	7.170	0.618	0.468	0.723	0.838	0.327	0.398	0.635	0.857	1.052	1.116	1.224	1.351	4/4 (4)
G194-22	9.889	-0.017	-0.101	0.168	0.484	0.270	0.256	0.440	0.659	0.814	0.869	0.891	0.951	4/3 (2)
- 3°2333	5.714	0.168	0.086	0.281	0.527	0.252	0.245	0.417	0.569	0.706	0.751	0.799	0.872	4/4 (4)
HD 74000	9.772	-0.059	-0.131	0.098	0.440	0.241	0.217	0.407	0.599	0.709	0.818	0.867	...	4/3 (0)
G115-22	11.121	0.183	0.039	0.355	0.636	0.321	0.309	0.504	0.758	0.933	0.991	1.086	...	4/2 (3)
+25°1981	9.404	-0.004	-0.072	0.115	0.336	0.192	0.170	0.310	0.481	0.591	0.641	0.664	0.971	4/4 (3)
+42°1922	8.874	1.312	1.116	1.385	1.136	0.308	0.609	0.898	1.186	1.427	1.542	1.677	1.904	4/4 (4)
-12°2669D	10.336	-0.069	-0.089	0.084	0.323	0.182	0.156	0.297	0.358	0.468	0.523	0.529	...	4/6 (0)
G46-5	11.477	0.575	0.404	0.735	0.878	0.363	0.386	0.624	0.890	1.058	1.140	1.304	...	4/4 (0)
G114-26	9.766	-0.007	-0.056	0.185	0.508	0.288	0.266	0.459	0.605	0.792	0.863	0.893	1.094?	4/4 (2)
G115-49	11.793	0.000	-0.133	0.163	0.516	0.280	0.266	0.482	0.513	0.733	0.813	0.880	...	4/3 (0)
+9°2190	11.307	-0.035	-0.106	0.098	0.397	0.230	0.183	0.393	0.511	0.651	0.735	0.824	...	4/4 (0)
G48-29	10.627	-0.050	-0.122	0.074	0.382	0.231	0.188	0.362	0.551	0.712	0.696	0.820	...	4/3 (0)
HD 84937	8.449	-0.040	-0.109	0.098	0.403	0.228	0.211	0.389	0.570	0.705	0.752	0.791	1.065?	4/4 (2)
+44°1910	11.105	0.044	-0.004	0.141	0.457	0.280	0.212	0.408	0.600	0.676	0.826	0.815	...	4/3 (0)
+23°2207	5.981	0.197	0.115	0.326	0.566	0.264	0.259	0.420	0.611	0.748	0.804	0.848	0.931	4/4 (4)
G119-32	10.406	-0.019	-0.097	0.184	0.536	0.266	0.254	0.458	0.697	0.861	0.897	0.974	0.892	4/4 (3)
G196-47	12.794	0.173	0.050	0.351	0.626	0.321	0.344	0.541	...	...	...	...	...	5/0 (0)
+21°2247	8.441	-0.037	-0.082	0.168	0.484	0.259	0.260	0.445	0.682	0.829	0.884	0.930	1.176	5/4 (4)
G10-4	11.577	0.364	0.211	0.464	0.803	0.398	0.366	0.642	...	...	...	...	...	4/0 (0)
+36°2165	9.957	0.013	-0.044	0.148	0.444	0.250	0.230	0.376	0.593	0.715	0.794	0.875	1.040?	4/4 (2)
+26°2251	10.535	0.072	0.022	0.242	0.541	0.269	0.258	0.442	0.505	0.680	0.724	0.776	...	4/3 (0)
+51°1696	10.063	0.163	0.060	0.302	0.646	0.330	0.286	0.510	0.690	0.895	0.911	0.978	0.792	2/4 (3)
BS 4550	6.626	0.556	0.419	0.738	0.873	0.348	0.390	0.655	0.894	1.099	1.183	1.300	1.430	55/48 (48)
G13-9	10.115	-0.030	-0.065	0.096	0.402	0.223	0.223	0.374	0.624	0.738	0.819	0.836	-0.038?	4/4 (3)
G11-44	11.157	-0.005	-0.081	0.164	0.466	0.280	0.214	0.426	0.664	0.812	1.042	0.875	...	4/3 (0)
HD 106038	10.285	0.026	-0.043	0.189	0.502	0.267	0.242	0.455	0.616	0.768	0.793	0.879	...	4/4 (0)

TABLE 1 - Continued

Name	52	33-52	35-52	37-52	40-52	45-52	52-58	52-63	52-72	52-80	52-86	52-99	52-110	NB/NR
HD 108177	9.811	-0.058	-0.123	0.140	0.460	0.261	0.241	0.437	0.583	0.777	0.804	0.799	1.330?	4/4 (3)
+40°2570	6.129	0.223	0.128	0.388	0.620	0.268	0.282	0.481	0.684	0.847	0.896	0.981	1.062	4/3 (3)
G60-48	11.403	0.009	-0.053	0.170	0.547	0.308	0.235	0.430	0.740	0.815	0.914	0.984	...	4/4 (0)
-9°3595	7.776	0.809	0.628	0.937	0.934	0.345	0.420	0.683	0.910	1.117	1.196	1.324	1.463	4/4 (4)
+10°2519	8.918	0.389	0.256	0.488	0.692	0.311	0.330	0.556	0.743	0.900	0.968	1.065	1.000	4/4 (4)
G14-45D	11.192	1.417	1.147	1.415	1.230	0.323	0.664	0.951	1.305	1.591	1.702	1.868	2.152?	4/3 (1)
+34°2476	10.188	-0.025	-0.084	0.108	0.414	0.243	0.210	0.393	0.587	0.720	0.769	0.817	1.208?	4/5 (3)
G65-22	11.786	0.529	0.403	0.657	0.797	0.354	0.307	0.604	...	...	...	...	...	4/0 (0)
G64-37	11.201	-0.010	-0.082	0.154	0.422	0.264	0.143	0.334	...	...	...	...	...	3/0 (0)
-13°3834	10.810	0.215	0.098	0.357	0.664	0.343	0.282	0.514	0.655	0.867	0.919	1.056	...	3/3 (0)
+1°2920	6.414	0.384	0.293	0.551	0.722	0.305	0.320	0.536	0.733	0.907	0.965	1.046	1.183	5/4 (4)
+30°2536	4.579	0.053	0.010	0.182	0.391	0.192	0.200	0.345	0.437	0.564	0.602	0.613	0.653	5/4 (4)
G66-22	10.611	0.456	0.399	0.680	0.828	0.351	0.375	0.623	0.867	1.062	1.107	1.275	...	4/3 (0)
+26°2606	9.827	-0.055	-0.124	0.139	0.457	0.275	0.224	0.412	0.561	0.718	0.771	0.807	...	4/5 (0)
-8°3858	9.698	0.587	0.465	0.693	0.818	0.326	0.372	0.624	0.816	1.016	1.078	1.192	...	4/4 (0)
-21°4009	8.655	0.208	0.078	0.274	0.599	0.312	0.281	0.497	0.721	0.878	0.957	1.055	1.078	2/4 (4)
+25°2873	5.012	0.159	0.106	0.287	0.491	0.221	0.236	0.397	0.538	0.657	0.692	0.731	0.759	4/4 (0)
-15°4041	9.669	0.845	0.735	1.023	1.009	0.375	0.459	0.757	1.051	1.261	1.352	1.510	1.849	4/5 (4)
-15°4042	9.292	0.600	0.462	0.782	0.893	0.365	0.401	0.672	0.967	1.172	1.261	1.370	1.489	4/4 (3)
G15-24	11.611	0.248	0.088	0.368	0.637	0.335	0.308	0.514	0.782	0.896	0.910	1.069	...	4/2 (0)
-10°4149	7.322	0.078	-0.006	0.181	0.517	0.315	0.255	0.478	0.662	0.821	0.907	0.995	1.077	4/4 (4)
+42°2667	10.007	0.034	-0.040	0.208	0.498	0.272	0.240	0.453	0.666	0.782	0.856	0.903	...	4/4 (0)
+39°2947	6.871	0.620	0.490	0.759	0.857	0.336	0.388	0.646	0.872	1.052	1.131	1.231	1.382	4/4 (4)
+39°2950	8.951	1.250	1.181	1.446	1.181	0.319	0.590	0.905	1.212	1.440	1.524	1.674	1.920	4/4 (4)
G168-42	11.701	0.497	0.345	0.629	0.801	0.374	0.371	0.636	...	...	...	...	...	4/0 (0)
G180-58	11.571	0.354	0.198	0.460	0.766	0.386	0.335	0.643	0.903	1.129	1.218	1.331	...	4/5 (0)
-3°3968	9.796	0.545	0.371	0.697	0.842	0.347	0.394	0.671	0.926	1.129	1.220	1.355	1.439	4/4 (2)
+37°2804	8.671	0.891	0.824	1.075	0.990	0.337	0.447	0.697	0.942	1.150	1.207	1.303	1.530	5/4 (3)
+43°2659	6.971	0.442	0.330	0.530	0.694	0.301	0.321	0.552	0.741	0.898	0.958	1.037	1.082	4/4 (4)
+17°3154	9.288	0.400	0.298	0.527	0.681	0.299	0.312	0.548	0.711	0.871	0.893	1.002	1.387?	4/4 (3)

238

PHOTOMETRY OF SUBDWARF STARS

TABLE 1 - Continued

Name	52	33-52	35-52	37-52	40-52	45-52	52-58	52-63	52-72	52-80	52-86	52-99	52-110	NB/NR
+ 1°3421	7.073	0.289	0.194	0.401	0.625	0.285	0.312	0.520	0.710	0.850	0.918	0.985	1.064	4/4 (4)
G170-56	9.894	0.086	0.017	0.231	0.502	0.274	0.248	0.445	0.581	0.747	0.817	0.869	0.859?	4/4 (2)
+ 2°3375	10.042	-0.052	-0.111	0.155	0.459	0.275	0.254	0.444	0.638	0.802	0.851	0.930	...	4/4 (0)
+37°2926	8.534	0.261	0.170	0.404	0.618	0.292	0.290	0.496	0.719	0.883	0.903	0.977	1.106?	4/4 (4)
+25°3344	7.036	0.408	0.347	0.087	0.144	0.095	0.104	0.198	0.286	0.338	0.378	0.424	0.449	4/4 (4)
G20-15	10.724	0.240	0.128	0.374	0.625	0.344	0.306	0.581	0.751	0.965	1.055	1.225	...	4/4 (0)
G183-11D	9.848	-0.028	-0.110	0.140	0.438	0.253	0.235	0.401	0.586	0.725	0.796	0.807	0.941	4/4 (2)
G154-36	9.747	0.215	0.157	0.438	0.675	0.337	0.305	0.567	0.728	0.918	0.984	1.111	1.282?	2/4 (1)
+13°3683	10.740	0.299	0.199	0.384	0.675	0.386	0.354	0.632	0.900	1.104	1.210	1.345	...	4/4 (0)
G206-34D	11.499	-0.075	-0.220	-0.144	0.436	0.271	0.228	0.416	0.582	0.776	0.773	0.866	...	4/3 (0)
+20°3926	4.310	0.237	0.154	0.317	0.514	0.236	0.238	0.407	0.525	0.636	0.679	0.711	0.846	4/4 (3)
AC+20°1463-148	11.236	...	2.301	2.393	2.006	0.680	0.819	1.394	2.252	2.835	3.055	3.357	3.690	3/4 (3)
AC+20°1463-154	11.247	...	2.159	2.260	1.992	0.669	0.818	1.433	2.233	2.850	3.060	3.395	3.602	3/4 (3)
+41°3306	9.107	0.838	0.671	0.944	0.918	0.326	0.437	0.733	0.934	1.163	1.238	1.383	1.483	4/4 (3)
+11°3833	5.342	0.849	0.777	0.964	0.919	0.334	0.392	0.626	0.792	0.952	1.003	1.116	1.198	3/4 (4)
+10°4091	8.964	0.136	0.055	0.351	0.649	0.319	0.310	0.555	0.729	0.932	0.962	1.060	1.130	3/4 (4)
+ 5°4481	10.306	0.332	0.190	0.401	0.647	0.301	0.296	0.509	0.735	0.896	0.959	1.104	...	4/5 (0)
-21°5703	8.747	0.098	0.031	0.259	0.562	0.314	0.276	0.494	0.735	0.850	0.945	0.995	1.163	3/5 (4)
+41°3735	9.182	0.615	0.444	0.481	0.712	0.362	0.306	0.533	0.811	0.983	1.073	1.187	1.321	4/6 (5)
+ 9°4529	8.457	0.056	0.004	0.202	0.513	0.264	0.247	0.416	0.612	0.799	0.848	0.889	1.142?	4/5 (5)
- 9°5491	9.716	0.448	0.313	0.326	0.622	0.349	0.317	0.582	0.832	1.044	1.131	1.248	1.451	4/4 (4)
+17°4519	7.534	0.075	-0.004	0.235	0.541	0.270	0.265	0.458	0.650	0.814	0.845	0.906	0.992	4/4 (4)
G188-30	11.211	0.330	0.214	0.441	0.748	0.362	0.328	0.602	0.881	1.032	1.149	1.219	...	5/3 (0)
G126-62	9.589	0.032	-0.043	0.188	0.485	0.269	0.224	0.422	0.565	0.728	0.779	0.906	1.717?	4/5 (3)
G18-39	10.502	0.086	-0.054	0.182	0.505	0.267	0.210	0.406	0.576	0.728	0.808	0.876	...	3/4 (0)
- 8°5980	8.189	0.448	0.334	0.573	0.735	0.306	0.338	0.545	0.768	0.946	0.990	1.084	1.173	4/5 (5)
G28-43	10.121	0.402	0.285	0.552	0.784	0.326	0.380	0.639	0.894	1.094	1.171	1.289	1.586?	4/4 (1)
G190-15	11.236	0.188	0.083	0.378	0.708	0.384	0.346	0.593	0.856	1.053	1.151	1.277	...	4/3 (0)
-14°6437	8.297	0.019	-0.071	0.187	0.512	0.277	0.261	0.456	0.663	0.817	0.862	0.925	1.038	4/5 (5)
+26°4734	5.932	0.414	0.295	0.552	0.748	0.312	0.375	0.610	0.851	1.049	1.122	1.231	1.404	5/7 (6)

TABLE 2

13-COLOR PHOTOMETRY OF HYADES STARS

Name	52	33-52	35-52	37-52	40-52	45-52	52-58	52-63	58-72	58-80	58-86	58-99	58-110	NB/NR
H6	6.062	0.179	0.119	0.242	0.393	0.171	0.177	0.300	0.242	0.340	0.354	0.371	0.411	1/2
7	9.266	1.172	1.084	1.278	1.121	0.337	0.504	0.769	0.509	0.712	0.767	0.907	1.053	2/3
9	....	....	....	....	....	....	....	....	0.452	0.623	0.669	0.781	0.868	0/2
20	6.422	0.206	0.130	0.278	0.452	0.180	0.224	0.362	0.264	0.349	0.396	0.440	0.540	2/3
22	8.534	0.743	0.654	0.890	0.912	0.318	0.420	0.650	0.466	0.672	0.744	0.853	1.018	2/2
25	9.917	1.350	1.274	1.505	1.214	0.315	0.583	0.889	....	....	....	....	....	2/0
26	....	....	....	....	....	0.32	0.38	0.59	0.454	0.619	0.692	0.779	0.939	0/2
27	8.64	0.74	0.63	0.85	0.88	0.453	0.460	0.743	0.437	0.609	0.649	0.765	0.842	2/2
28	3.868	1.531	1.371	1.445	1.292	0.260	0.292	0.475	0.521	0.740	0.830	0.976	1.141	2/3
29	7.002	0.338	0.262	0.471	0.645	....	....	....	0.366	0.506	0.550	0.604	0.727	2/2
30	5.656	0.302	0.211	0.254	0.339	0.129	0.155	0.258	0.197	0.271	0.277	0.305	0.369	2/8
33	5.338	0.254	0.193	0.230	0.269	0.100	0.139	0.215	0.144	0.195	0.206	0.228	0.274	2/2
34	6.269	0.217	0.141	0.335	0.520	0.219	0.231	0.390	0.306	0.428	0.450	0.485	0.547	1/2
35	6.92	0.18	0.13	0.30	0.49	0.20	0.22	0.38	0.308	0.415	0.446	0.476	0.572	1/2
36	6.921	0.186	0.118	0.304	0.496	0.213	0.222	0.380	0.301	0.420	0.442	0.476	0.562	1/2
40	....	....	....	....	....	....	....	....	0.396	0.537	0.581	0.646	0.741	0/2
41	3.997	1.584	1.422	1.488	1.308	0.456	0.472	0.749	0.508	0.718	0.806	0.949	1.108	2/2
43	9.634	1.115	1.039	1.269	1.122	0.344	0.494	0.772	0.581	0.800	0.905	1.039	1.276	2/3
45	5.742	0.322	0.250	0.314	0.380	0.126	0.166	0.256	0.163	0.233	0.252	0.276	0.259	2/2
46	9.386	1.017	0.936	1.178	1.064	0.348	0.468	0.705	0.507	0.697	0.777	0.886	1.007	2/3
47	4.861	0.265	0.220	0.221	0.205	0.077	0.109	0.156	0.118	0.160	0.155	0.202	0.232	2/2
48	....	....	....	....	....	....	....	....	0.334	0.487	0.520	0.564	0.668	0/2
50	7.75	0.43	0.32	0.56	0.70	0.28	0.31	0.51	0.423	0.591	0.639	0.673	0.851	2/2
51	....	....	....	....	....	....	....	....	0.318	0.422	0.454	0.490	0.575	0/2
52	....	....	....	....	....	....	....	....	0.405	0.560	0.591	0.675	0.828	0/1
53	6.089	0.250	0.178	0.290	0.427	0.188	0.206	0.337	0.257	0.353	0.373	0.464	0.497	1/2
54	4.288	0.281	0.229	0.202	0.172	0.054	0.105	0.152	0.078	0.128	0.131	0.156	0.197	2/2
56	4.320	0.101	0.074	0.085	0.069	0.014	0.048	0.061	0.024	0.044	0.030	0.055	0.077	2/8
57	6.599	0.250	0.167	0.369	0.553	0.236	0.271	0.449	0.320	0.446	0.471	0.516	0.622	1/2
58	7.711	0.589	0.514	0.739	0.808	0.299	0.363	0.579	0.442	0.593	0.650	0.727	0.855	1/2
59	....	....	....	....	....	....	....	....	0.379	0.522	0.553	0.609	0.721	0/2

PHOTOMETRY OF SUBDWARF STARS

TABLE 2 - Continued

Name	52	33-52	35-52	37-52	40-52	45-52	52-58	52-63	58-72	58-80	58-86	58-99	58-110	NB/NR
H60	4.384	0.408	0.307	0.237	0.292	0.126	0.179	0.276	0.189	0.255	0.286	0.330	0.420	2/2
64	8.255	0.536	0.469	0.693	0.782	0.292	0.332	0.543	0.415	0.582	0.616	0.710	0.840	1/2
65	....	....	....	....	....	....	....	....	0.369	0.504	0.539	0.589	0.710	0/2
68	5.966	0.254	0.183	0.275	0.384	0.154	0.168	0.286	0.235	0.325	0.315	0.384	0.489	1/3
69	8.806	0.749	0.636	0.866	0.880	0.309	0.384	0.612	0.437	0.609	0.656	0.777	0.946	2/2
70	3.781	1.698	1.520	1.576	1.384	0.467	0.484	0.754	0.510	0.726	0.845	0.977	1.163	2/2
71	4.090	1.476	1.306	1.407	1.266	0.439	0.462	0.727	0.503	0.711	0.806	0.951	1.122	11/4
72	3.475	0.313	0.252	0.205	0.209	0.060	0.094	0.173	0.135	0.177	0.175	0.223	0.256	13/3
73	8.009	0.447	0.340	0.568	0.705	0.279	0.319	0.514	0.434	0.578	0.626	0.692	0.780	1/2
77	7.152	0.245	0.164	0.373	0.554	0.239	0.272	0.447	0.346	0.488	0.537	0.581	0.640	1/2
79	9.162	0.915	0.864	1.094	1.018	0.324	0.434	0.680	0.489	0.660	0.725	0.832	0.891	2/1
82	4.840	0.275	0.216	0.218	0.193	0.069	0.109	0.146	0.082	0.135	0.135	0.175	0.167	2/2
85	6.607	0.214	0.137	0.320	0.506	0.222	0.228	0.394	0.303	0.401	0.447	0.494	0.534	1/2
87	8.806	0.754	0.643	0.914	0.893	0.327	0.406	0.629	0.451	0.608	0.668	0.785	0.972	1/2
91	....	....	....	....	....	....	....	....	0.561	0.779	0.859	0.986	1.176	0/2
92	....	....	....	....	....	....	....	....	0.479	0.620	0.672	0.787	0.930	0/2
94	6.706	0.195	0.119	0.295	0.493	0.216	0.224	0.382	....	....	....	....	....	1/0
95	4.765	0.265	0.200	0.230	0.271	0.096	0.113	0.190	0.140	0.199	0.220	0.234	0.291	2/2
97	8.10	0.46	0.39	0.61	0.74	0.27	0.31	0.49	....	....	....	....	....	2/0
104	4.329	0.257	0.204	0.190	0.159	0.048	0.082	0.109	0.065	0.100	0.108	0.137	0.176	2/2
108	4.721	0.274	0.225	0.218	0.190	0.062	0.087	0.111	0.107	0.166	0.169	0.206	0.235	2/2
117	9.974	1.403	1.330	1.555	1.307	0.369	0.627	0.953	0.640	0.887	1.018	1.205	1.408	1/2
123	5.153	0.294	0.227	0.242	0.261	0.103	0.121	0.181	0.118	0.183	0.197	0.235	0.388	3/2
129	4.670	0.318	0.27	0.224	0.197	0.076	0.097	0.137	....	....	....	....	....	1/0
141	4.565	0.356	0.265	0.239	0.274	0.119	0.162	0.251	0.154	0.241	0.266	0.310	0.360	2/2
169	4.159	0.265	0.225	0.206	0.209	0.082	0.086	0.146	0.125	0.202	0.210	0.261	0.336	3/1
175	10.580	1.392	1.392	1.588	1.304	0.350	0.623	0.950	0.605	0.834	0.932	1.078	1.056	1/3
176	9.311	1.167	1.060	1.302	1.136	0.319	0.565	0.850	0.556	0.765	0.859	0.987	1.165	3/4
181	10.768	1.798	1.728	1.919	1.515	0.307	0.791	1.111	0.693	0.965	1.056	1.269	1.369	2/3

TABLE 3

MILD SUBDWARFS WHOSE 13-COLOR
PHOTOMETRY WAS NOT TAKEN AT
SAN PEDRO MARTIR, B. C.

Name	45 − 63	S_p
BS 77	0.806	G2V
BS 219D	0.795	G0V
BS 1008	0.945	G5V
BS 6752D	1.102	K0V
BS 6927	0.714	F7V
BS 8181	0.721	F8V

110 color contains considerable uncertainty, and in column 15 the number in parentheses gives the number of 1.1μ observations; in Table 2 this number always equals NR.

In Table 3 are listed the bright star numbers (Hoffleit 1964), 45 − 63 indices, and spectral types of six additional stars with moderately large ultraviolet excesses. These stars are taken from the subdwarf list of Johnson et al. (1968), and their 13-color photometry has been obtained from Mitchell and Johnson (1969) and from Johnson and Mitchell (1975). These six stars were not observed at

'SPM', but their photometry is included in the following analyses.

The quality of the SPM 13-color data seems to be good, comparable in quality to the Catalina observations (Johnson et al. 1967, Mitchell and Johnson 1969), which define this photometric system. Schuster (1976a) gave the probable errors for the standard stars observed at SPM. Also in Table 4 are listed the probable errors of a single observation for the subdwarfs grouped according to brightness — 52 magnitudes for 8C photometry and 58 magnitudes for 6RC photometry. All subdwarfs have been included in these average probable errors except for two very southern ones which have been dropped from the brightest groups, and six very red subdwarfs which have been dropped from the faintest 8C group. These stars were dropped so that the results of Table 4 are representative of the F and G-type subdwarfs. These results indicate that the 'SPM' 6RC photometry is a good as, or perhaps better than, the Catalina results and that, except for the 52 magnitude and the 33 − 52 color, the 8C results are quite similar in quality. A less stable standard lamp is the reason for the larger 52 errors at 'SPM' and a dustier observing site (dustier optics) explains the larger 33 − 52 errors.

TABLE 4

PROBABLE ERRORS OF A SINGLE OBSERVATION FOR THE SUBDWARFS

Color	<6.999	7.000-7.999	8.000-8.999	9.000-9.999	10.000-10.999	>11.000
52	0.030	0.028	0.026	0.022	0.034	0.028
33-52	0.018	0.019	0.022	0.028	0.031	0.039
35-52	0.013	0.014	0.021	0.020	0.024	0.033
37-52	0.013	0.013	0.017	0.018	0.020	0.027
40-52	0.009	0.012	0.014	0.014	0.015	0.016
45-52	0.009	0.013	0.011	0.012	0.012	0.014
52-58	0.012	0.012	0.011	0.013	0.017	0.018
52-63	0.018	0.013	0.013	0.017	0.020	0.027
58	0.027	0.028	0.026	0.025	0.031	0.027
58'	0.022	0.021	0.029	0.037	0.035	0.044
58-72	0.017	0.024	0.028	0.033	0.033	0.050
58-80	0.017	0.021	0.027	0.031	0.029	0.046
58-86	0.019	0.015	0.030	0.030	0.033	0.045
58-99	0.022	0.020	0.029	0.033	0.036	0.057
58-110	0.045	0.053	0.088	0.098	....	....
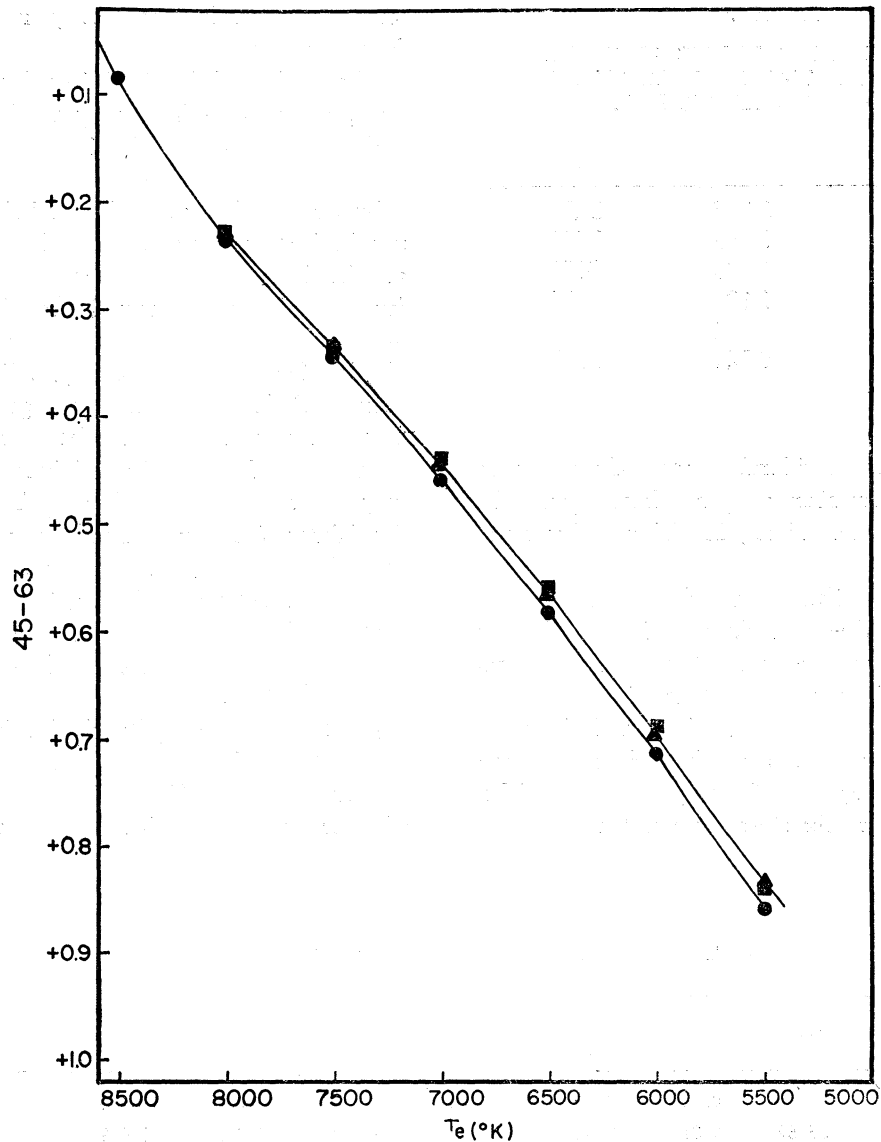
FIG. 1. Theoretical *45-63* versus Te curves. Filled circles are for solar abundance, triangles for 0.1 solar abundance, and squares 0.01. Log g = 4.0.

The subdwarfs −33°4113, G38-1, AC + 20° 1463 − 148 and AC + 20°1463 − 154 have ultra-violet errors significantly larger than those given in Table 4. For −33°4113 this has resulted because it was observed at very large air masses. The others are all red subdwarfs with spectral types of sdK5 or sdM2 and so are much fainter in the ultraviolet than F and G subdwarfs with comparable visual magnitudes. G99 − 31D, G115 − 49, +25°2251,

G60 − 48 and G15 − 24 are subdwarfs whose 6RC observations show probable errors significantly larger than those of Table 4 or whose 6RC observations were selectively averaged. For G99 − 31D these problems resulted because of the contamination of a nearby star. The others are all fainter than magnitude 52 = 10.5, and the scatter in the 6RC observations probably results from small instabilities in the phototube or electronics.
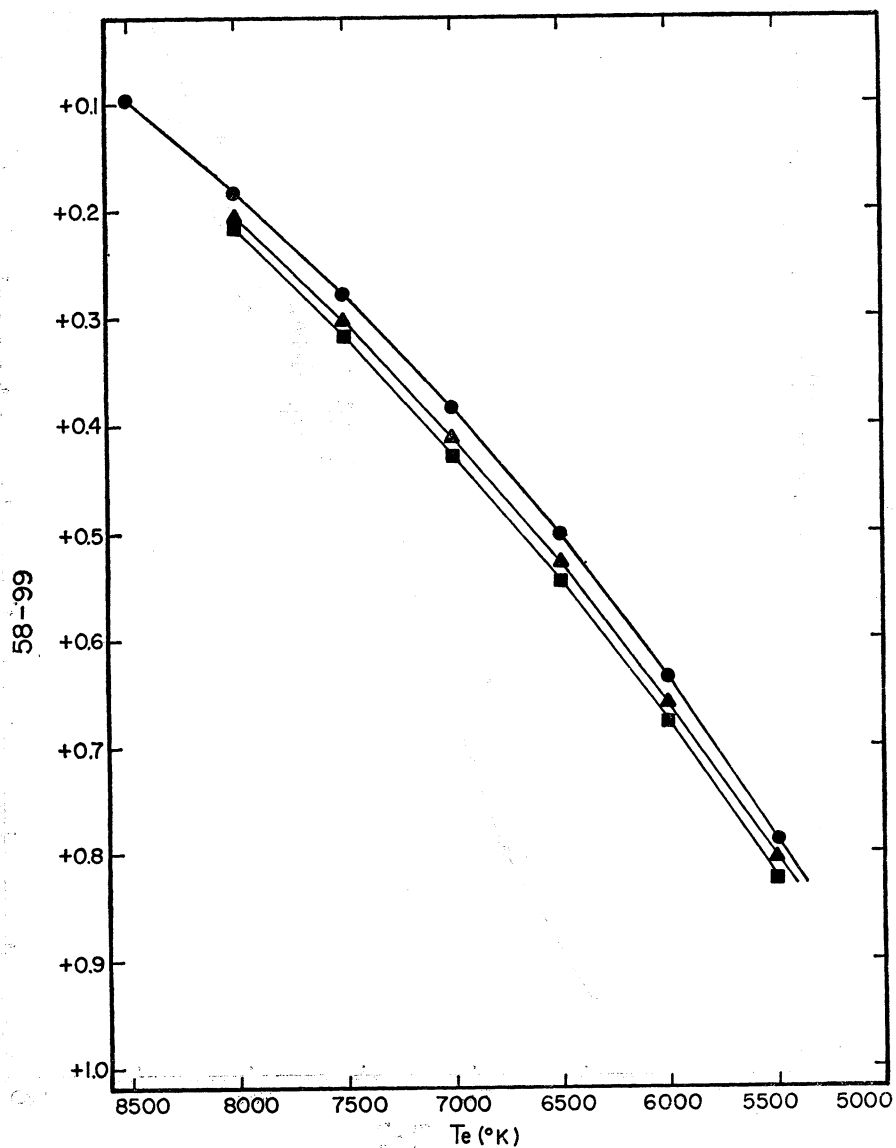
Fig. 2.   Theoretical *58-99* versus Te curves. The symbols are the same as in Figure 1. Log g =   4.5.

III. MEAN HYADES COLORS

Using the Hyades photometry of Table 2, mean Hyades colors, as a function of spectral type and as a function of the *45 — 63* index have been obtained. Of the 60 Hyades stars in Table 2 excellent spectral types are available for 51 from the work of Morgan and Hiltner (1965). Only these spectral types of Morgan and Hiltner have been used in deriving the mean colors, and only main sequence stars have been used; all evolved stars and all Am

stars have been excluded. The mean colors (versus spectral type) have been derived by merely hand drawing lines of best fit through 12 different spectrum-color diagrams. To make maximum use of the available data, since some of the Hyades stars have 8C photometry but do not have an accurate spectral type, the mean colors were also derived as a function of *45 — 63*. Twelve color-color plots (13-color index versus *45 — 63*) were made for this purpose. The two sets of mean colors were tied
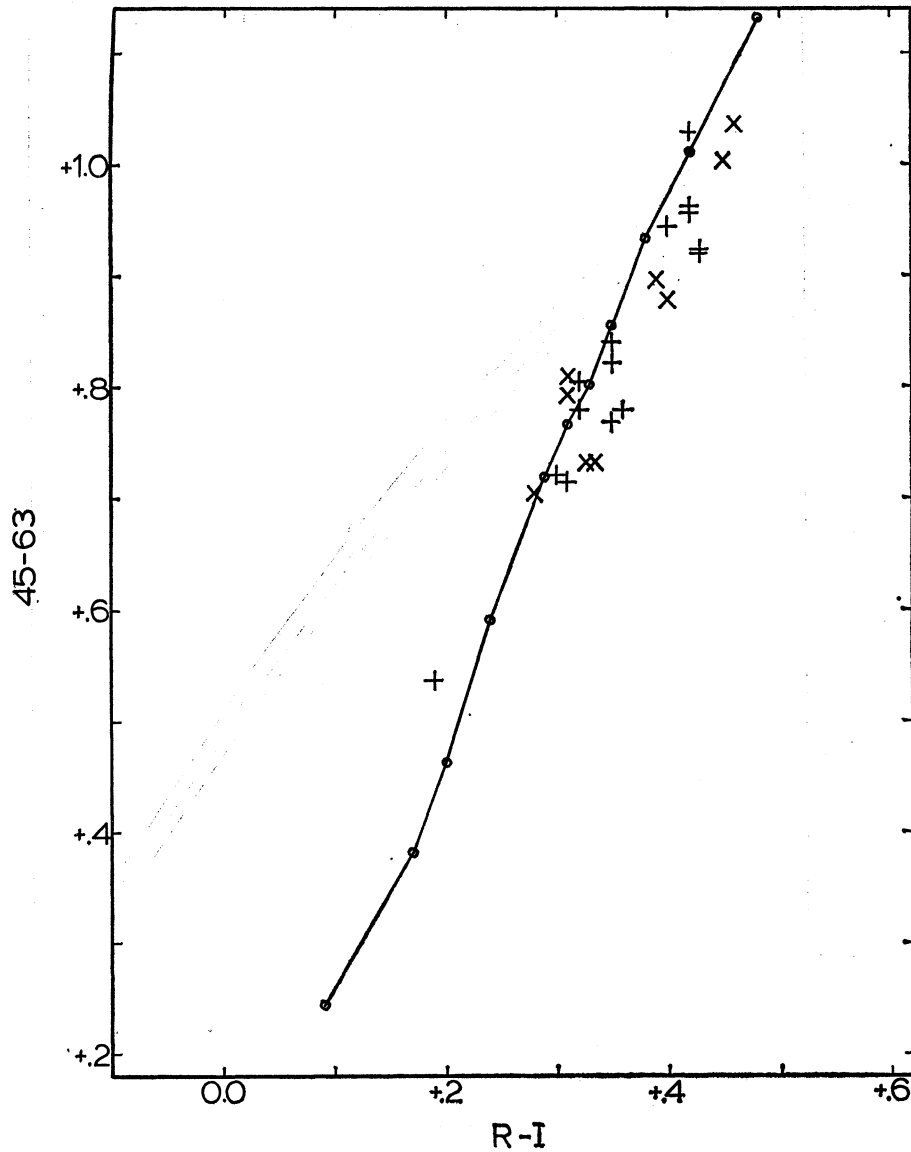
FIG. 3. *45-63* versus R-I. The circles and solid line represent the mean Hyades colors, the plus signs mild subdwarfs and the X's extreme subdwarfs.

together using a *45 − 63* versus spectray type diagram, and the combined mean colors as a function of both spectral type and *45 − 63* are given in Table 5. Comparing the two independently derived sets of mean colors has given us a good idea for the accuracy of Table 5. For spectral types A4 to K0 and for colors *35 − 52* to *52 − 99* the probable errors are of the order of, or less than, 0.01 magnitude. Colors *33 − 52* and *52 − 110* have

probable errors somewhat larger in the range 0.01 to 0.02. For spectral types K2 and K4 the probable errors may be twice those quoted above.

IV. THEORETICAL 13-COLOR PHOTOMETRY

The theoretical 13-color photometry used throughout this paper to obtain blanketing and gravity correc-
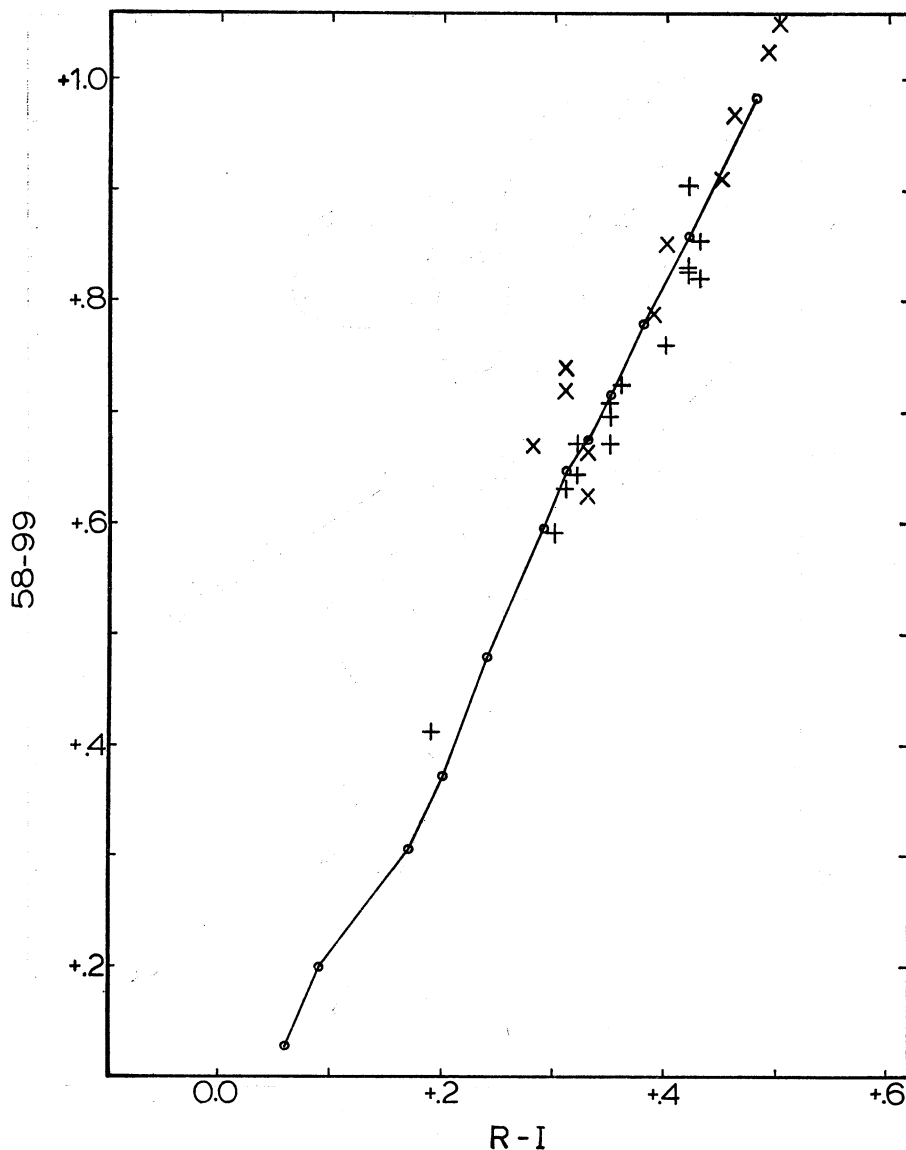
Fig. 4. *58-99* versus R-I. The symbols are the same as in Figure 3.

tions for the *45 − 63* temperature index and to provide theoretical blanketing and gravity-difference curves has come from Kurucz (1975). The flux-constant, line-blanketed model atmospheres which give the necessary stellar flux distributions were calculated using the ATLAS computer code as given and described by Kurucz (1970). Dr. Kurucz was so kind as to convolve the filter-detector response functions of the 13-color filters (Johnson *et al.* 1967 and Mitchell and Johnson 1969) with

the emergent flux per wavelength interval distributions of his models. The resulting theoretical colors were then normalized to the standard 13-color system by fitting a (9400, 3.95, 1×, 2) model to the 13-color observations of Vega (with four 8C and 36 6RC observations). The choice of these parameters for Vega has been discussed by Kurucz (1974). The resulting grid of theoretical 13-color photometry is like the *uvby* grid given by Relyea and Kurucz (1976) with a similar range in effective
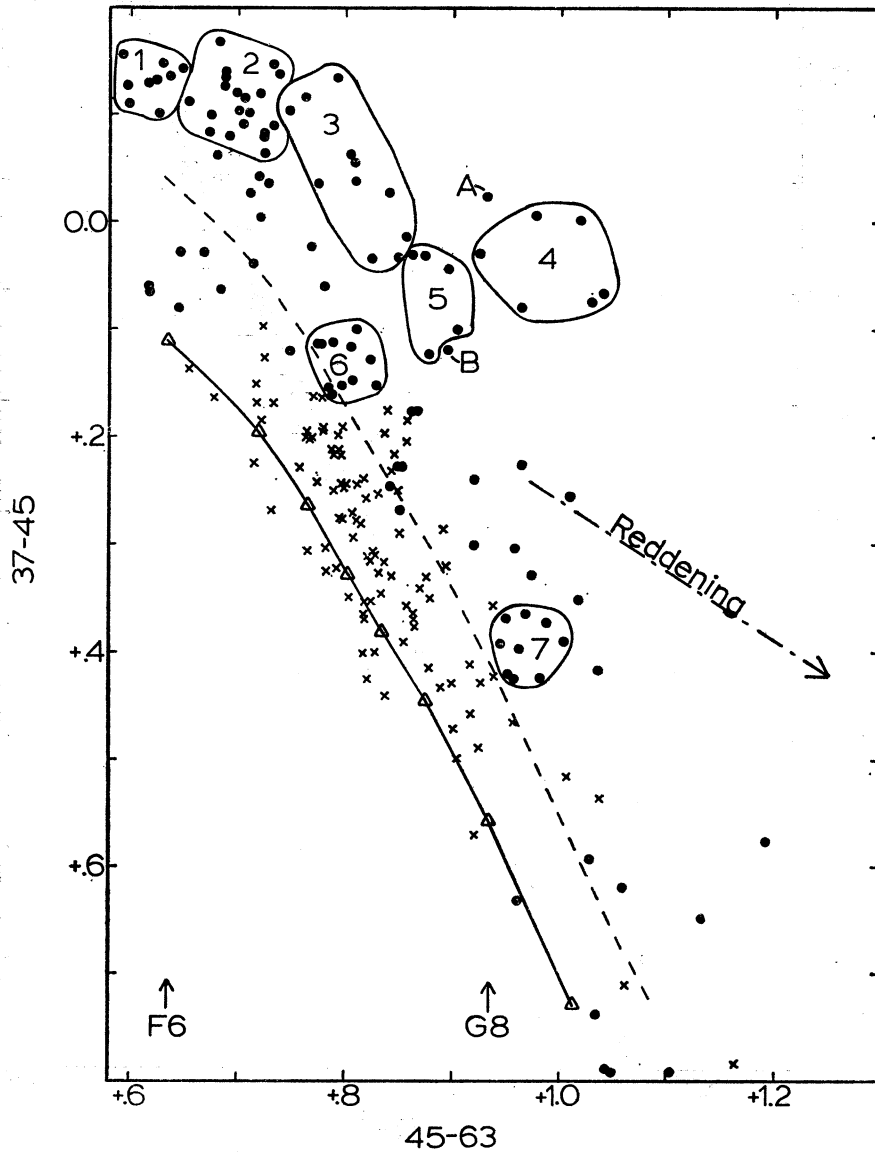
Fig. 5. *37-45* versus *45-63*. Filled circles are for subdwarfs, X's for solar-type stars, and the triangles and solid line for the Hyades mean colors. The other features are explained in the text.

temperatures, gravities, and metal contents; the 13-color grid will be published later.

The great usefulness of these models for the study of subdwarfs and for the comparison of metal-rich and metal-poor stars lies in the fact that they are blanketed models for the atmospheres of stars as cool as types F and G. The blanketing of approximately 900,000 atomic lines is included by

means of a statistical representation of the line opacities as described by Strom and Kurucz (1966) and by Kurucz (1970, 1974). The success of these models in producing theoretical *uvby* photometry to match a great amount of observational data is discussed by Relyea and Kurucz (1976). The only discrepancies are noted at cooler temperatures resulting from the use of the conventional mixing length

theory in the treatment of convection (Relyea and Kurucz 1976) and from the lack of molecular opacities in the models.

According to the observational results of Johnson and Mitchell (1968) the $45 - 63$ temperature index should be fairly independent of metallicity, and for this reason the $45 - 63$ index has been used to construct the blanketing curves of this paper. In following papers the indices $45 - 63$ and $58 - 99$ will be used to derive effective temperatures for the subdwarfs. Hence, at this point it is important to make some sort of independent check on the theoretical blanketing corrections for the $45 - 63$ and $58 - 99$ indices. In Figures 1 and 2 are plotted the $45 - 63$ and $58 - 99$ versus Te curves from the theoretical colors; curves are drawn for solar abundance (1×, for 0.1× and for 0.01×; the surface gravity is kept constant at log g = 4.0 in Figure 1 and at log g = 4.5 in Figure 2. In Figures 3 and 4 a direct observational check of the blanketing of $45 - 63$ and $58 - 99$ has been made by plotting the color-color diagrams, $45 - 63$ versus R − I and $58 - 99$ versus R − I, using mean Hyades colors and several mild and extreme subdwarfs. The mean Hyades colors come from Table 5 for $45 - 63$ and from Table 2 of Johnson et al. (1968) for R − I. The R − I values of the subdwarfs come from this last source and also from Eggen (1973); the Kron R − I values of Eggen have been transformed to the Johnson R − I system. The assumption that the broad-band index R − I is independent of the metallicity of a stellar atmosphere has been documented and used in a number of recent investigations (Johnson et al. 1968; Johnson and Mitchell 1968; Eggen 1973, 1974). A comparison of Figures 1, 2, 3, and 4 shows that the theoretical blanketing corrections for $45 - 63$ contain no errors greater than about 0.02 magnitude and the corrections for $58 - 99$ no errors greater than 0.03 or 0.04 magnitude. The comparisons also show that if the theoretical blanketing corrections are exact, R − I changes by +0.01 or +0.02 in going from a Hyades composition to a subdwarf composition.

V. BLANKETING CURVES

The work of Johnson and Mitchell (1968) indicated that the $37 - 45$, $45 - 63$ diagram should allow "nearly the maximum discrimination among stars of differing metal content". The $37 - 45$ index contains nearly the full blanketing effect, and, as we have confirmed above, $45 - 63$ is a good temperature index with a very small sensitivity to metallicity. In Figure 5 we have plotted the $37 - 45$, $45 - 63$ diagram for the subdwarfs, the Hyades mean colors, and early-G dwarfs (Schuster 1976a). The dot-dash line in Figure 5 is a reddening line; all reddening lines for the 8C photometry have been obtained from the work of Borgman (1961). The dashed line represents the locus with an ultraviolet excess, $\delta(37 - 45)$, of +0.15 where $\delta(37 - 45)$ is defined as the difference between the Hyades mean $37 - 45$ and a star's $37 - 45$ at constant $45 - 63$. We see that indeed the subdwarfs are well separated from the Hyades and from early-G field dwarfs and that the dashed line represents a reasonable criterion for selecting metal-poor stars in this temperature range ($0.60 < 45 - 63 < 1.04$) as suggested by Schuster (1976a). The only subdwarfs which lie below the dashed line, such as the group of six at approximately $45 - 63 = 0.65$ and $37 - 45 = +0.05$, have been called subdwarfs because their parallaxes placed them below the main sequence in a (Mbol, Te) diagram, or some equivalent color-magnitude diagram, and not because they have been classified subdwarfs spectroscopically. We note in Figure 5 that the more extreme subdwarfs can easily have excesses, $\delta(37 - 45)$ of + 0.4 or + 0.5.

The luminosity (or gravity) sensitivity of the $37 - 45$, $45 - 63$ diagram has been discussed previously (Schuster 1976a and 1976b). This diagram is not very sensitive to luminosity for the range $0.6 < 45 - 63 < 0.95$ with nearly all field subgiants, giants, and supergiants lying within 0.15 magnitude of the mean Hyades main sequence, nearly in the same region of the diagram as the field dwarfs. (We argue that exceptions such as BS5409 with Sp = G2III, $45 - 63 = 0.900$ and $\delta(37 - 45) > 0.15$ and BS98 with Sp = G2IV, $45 - 63 = 0.837$, and $\delta(37 - 45) > 0.15$ are in fact both metal-poor and evolved.) For $45 - 63 > 0.95$ the $37 - 45$ color becomes more sensitive to luminosity; increasing luminosity mimics decreasing metallicity. In general then for $0.6 < 45 - 63 < 0.95$ stars lying above the dashed line in Figure 5 can be selected as candidates for being metal poor

TABLE 5

MEAN HYADES COLORS

Sp	45-63	33-52	35-52	37-52	40-52	45-52	52-58	52-63	52-72	52-80	52-86	52-99	52-110
A4	0.108	0.178	0.150	0.140	0.102	0.026	0.062	0.074	0.104	0.130	0.128	0.154	0.180
A6	0.200	0.272	0.221	0.208	0.184	0.062	0.095	0.131	0.185	0.226	0.231	0.260	0.292
A8	0.291	0.283	0.216	0.232	0.258	0.098	0.125	0.192	0.264	0.319	0.330	0.360	0.403
F0	0.382	0.274	0.188	0.251	0.330	0.132	0.156	0.256	0.346	0.415	0.430	0.462	0.516
F2	0.464	0.228	0.154	0.262	0.391	0.164	0.183	0.309	0.419	0.500	0.522	0.556	0.619
F4	0.548	0.196	0.127	0.288	0.454	0.194	0.211	0.360	0.487	0.585	0.615	0.654	0.726
F6	0.634	0.203	0.134	0.334	0.524	0.224	0.245	0.409	0.563	0.675	0.718	0.761	0.846
F8	0.719	0.310	0.217	0.445	0.614	0.250	0.280	0.461	0.640	0.778	0.821	0.877	0.971
G0	0.766	0.406	0.306	0.532	0.680	0.269	0.304	0.492	0.696	0.845	0.883	0.951	1.066
G2	0.802	0.474	0.370	0.610	0.722	0.283	0.324	0.519	0.730	0.886	0.924	1.000	1.124
G4	0.835	0.529	0.434	0.676	0.761	0.295	0.342	0.543	0.758	0.918	0.959	1.043	1.168
G6	0.875	0.605	0.512	0.750	0.810	0.306	0.364	0.574	0.793	0.959	1.005	1.094	1.221
G8	0.934	0.742	0.640	0.873	0.889	0.318	0.394	0.618	0.846	1.018	1.072	1.174	1.306
K0	1.012	0.909	0.820	1.056	0.991	0.328	0.442	0.680	0.937	1.117	1.193	1.300	1.450
K2	1.132	1.135	1.068	1.303	1.128	0.334	0.518	0.782	1.070	1.281	1.375	1.501	1.692:
K4	1.315	1.472	1.460	1.658	1.327	0.337	0.663	1.032	1.289	1.552	1.645	1.809	1.963:

while for $45 - 63 > 0.95$ evolving stars can be confused with metal-poor ones.

In Figure 5 seven groups of subdwarfs, have been encircled and numbered. (The stars marked 'A' and 'B' will be discussed later). The averaged blanketing curves of these groups will be obtained in the following manner. Many of the early-G dwarfs and several of the subdwarfs in Figure 5 have had their compositions measured spectroscopically. (For example, see Morel et al. 1976). By composition we are referring primarily to the logarithmic iron to hydrogen ratio, [Fe/H]. Using the stars with measured compositions we have estimated the compositions of all stars plotted in Figure 5; a star's $\delta(37 - 45)$ depends very strongly upon its composition. Then using Figure I we have corrected a subdwarf's $45 - 63$ to $(45 - 63)s$, the value it would have with a solar composition. The composition estimates made from Figure 5 need not be very accurate since the blanketing corrections for $45 - 63$, as shown in Figure 1, are all small, usually $+0.02$ or smaller. Now, assuming that $(45 - 63)s$ is the same as for a Hyades composition, which is not in error by more than a few thousandths of a magnitude, we interpolate in Table 5 for the Hyades mean colors with the same Te as the subdwarf. The differences between these Hyades mean colors and the subdwarf's observed colors are plotted versus the effective wavelengths of the filters to give a blanketing curve.

In all of these analyses no reddening corrections have been applied to the subdwarf photometry. Most subdwarfs lie within 100 parsecs and so require little or no reddening corrections. A few may

be as far away as 250 parsecs and are probably slightly reddened. Reddening-free indices can be derived in the manner of Stromgren (1966). For example, using the results of Borgman (1961) and of Whitford (1958) we find that $C = (37 - 45) - 0.6(45 - 63)$ can be used as a reddening-free composition parameter which still retains a large sensitivity to metallicity. But, all suitable 13-color temperature indices when dereddened lose their temperature sensitivity. Alternatively statistical reddening corrections exist, as shown by Sandage's (1964) discussion of the use of Parenago's (1940) reddening equation, but these are of no use for analyzing individual stars and of limited use for analyzing small numbers of stars as in the seven groups of Figure 5.

The lowest effective temperature for the stellar atmospheric models of Kurucz is $5500°$ which corresponds to $45 - 63 = 0.86$ at a solar abundance and 0.84 at 0.01 solar abundance. Hence we cannot directly use these models to obtain blanketing corrections for the stars in groups 4, 5 and 7 of Figure 5. However, in Figures 1 and 3 we see clear evidence that the blanketing corrections of $45 - 63$ remain fairly constant over the interval $+0.7 < 45 - 63 < +1.0$. So the blanketing corrections of the models have been extrapolated with good confidence to $45 - 63 \sim +1.0$ which corresponds to Te $\sim 5250°$.

In Figures 6 and 7 are plotted the observational blanketing curves of the seven groups of subdwarfs, and in Table 6 are given the mean characteristics of these groups. The compositions of Table 6 were obtained in the manner mentioned above, using

TABLE 6

THE GROUPS OF SUBDWARFS IN FIGURES 6 AND 7

Group No.	No. of Stars	$(T_e)_{Ave}$	$[Fe/H]_{Ave}$	$\Delta(37 - 52)_{Ave}$
1	9	6210	$- 1.43$	0.235
2	18	6000	$- 1.38$	0.299
3	11	5730	$- 1.48$	0.391
4	6	5170	$< - 2.0$	0.635
5	5	5510	$- 1.38$	0.422
6	9	5750	$- 0.37$	0.193
7	9	5320	$- 0.63$	0.247
BS 4550	1	5180	$- 1.30$	0.342
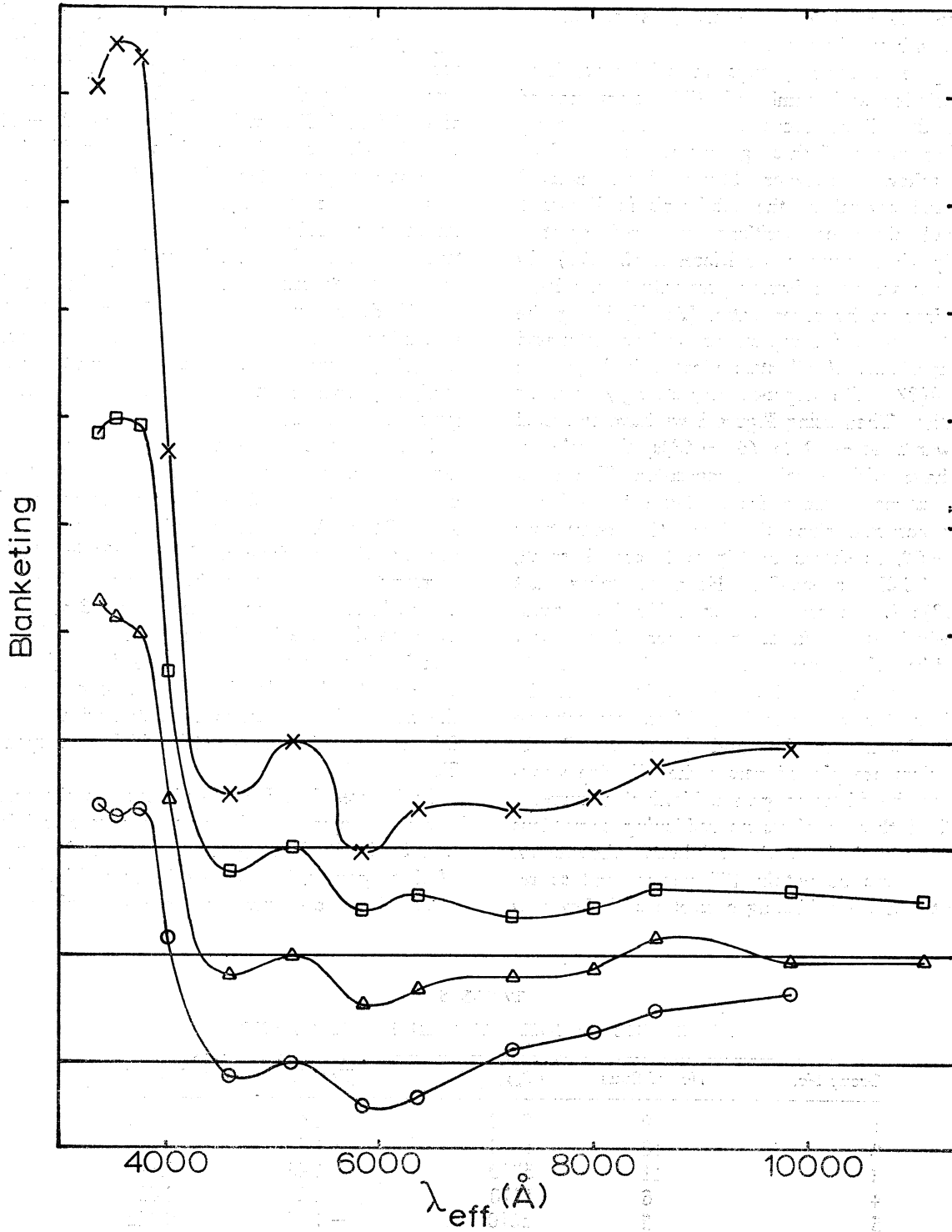
Fig. 6. The average observational blanketing curves for the subdwarfs of groups 1 (circles), 2 (triangles), 3 (squares), and 4 (crosses). The shift of the horizontal lines and the scale of the ordinate axis are both 0.1 magnitude.
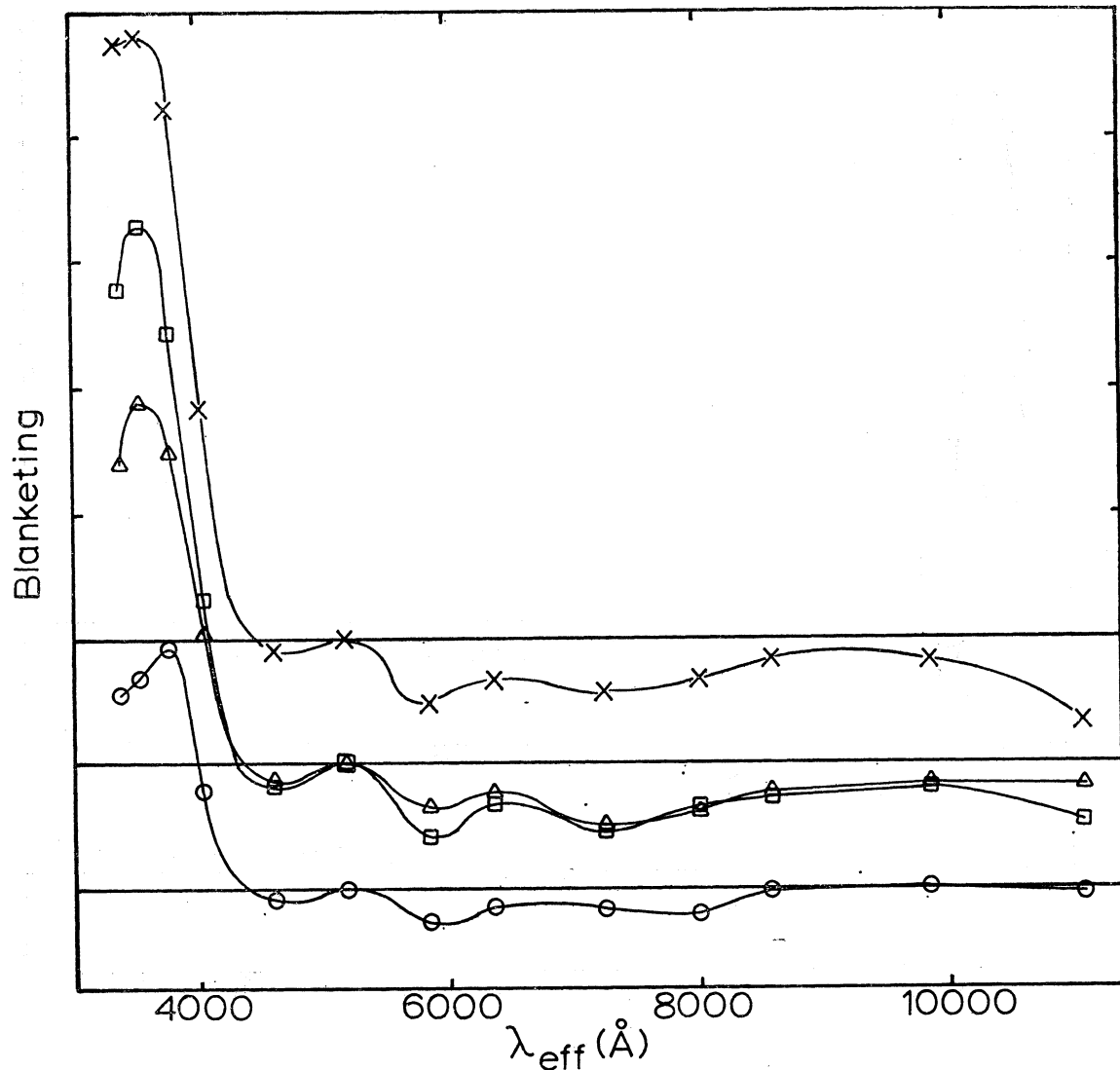
Fig. 7. The average observational blanketing curves for the subdwarfs of groups 5 (crosses) 6 (circles) and 7 (triangles). The squares give the blanketing curve for BS4550, which is one of the subdwarfs from group 7 and is also a thirteen-color standard. The shift of the horizontal lines and the scale of the ordinate axis are both 0.1 magnitude.

the ultraviolet excesses from Figure 5, and the temperatures come from Figures 1 and 2 and from observational calibrations of $45 - 63$ and $58 - 99$ to be given in a later paper. We have plotted only average blanketing curves since the aim is to study the sensitivity of the 13-color indices; later the individual curves of some interesting subdwarfs will be given. In Figures 6 and 7 the straight horizontal lines represent the energy distribution of a Hyades main sequence star while the plotted points represent the relative distribution of the subdwarfs. The curves which pass through the points are drawn only to help the eye detect relationships and do *not* represent interpolations of the data. To a good first approximation we can assume that these observational blanketing curves show only effects of metallicity since the subdwarfs have compositions greatly different from the Hyades, but small surface gravity effects are also included as will be discussed later. In Figure 8 are plotted theoretical blanketing curves;
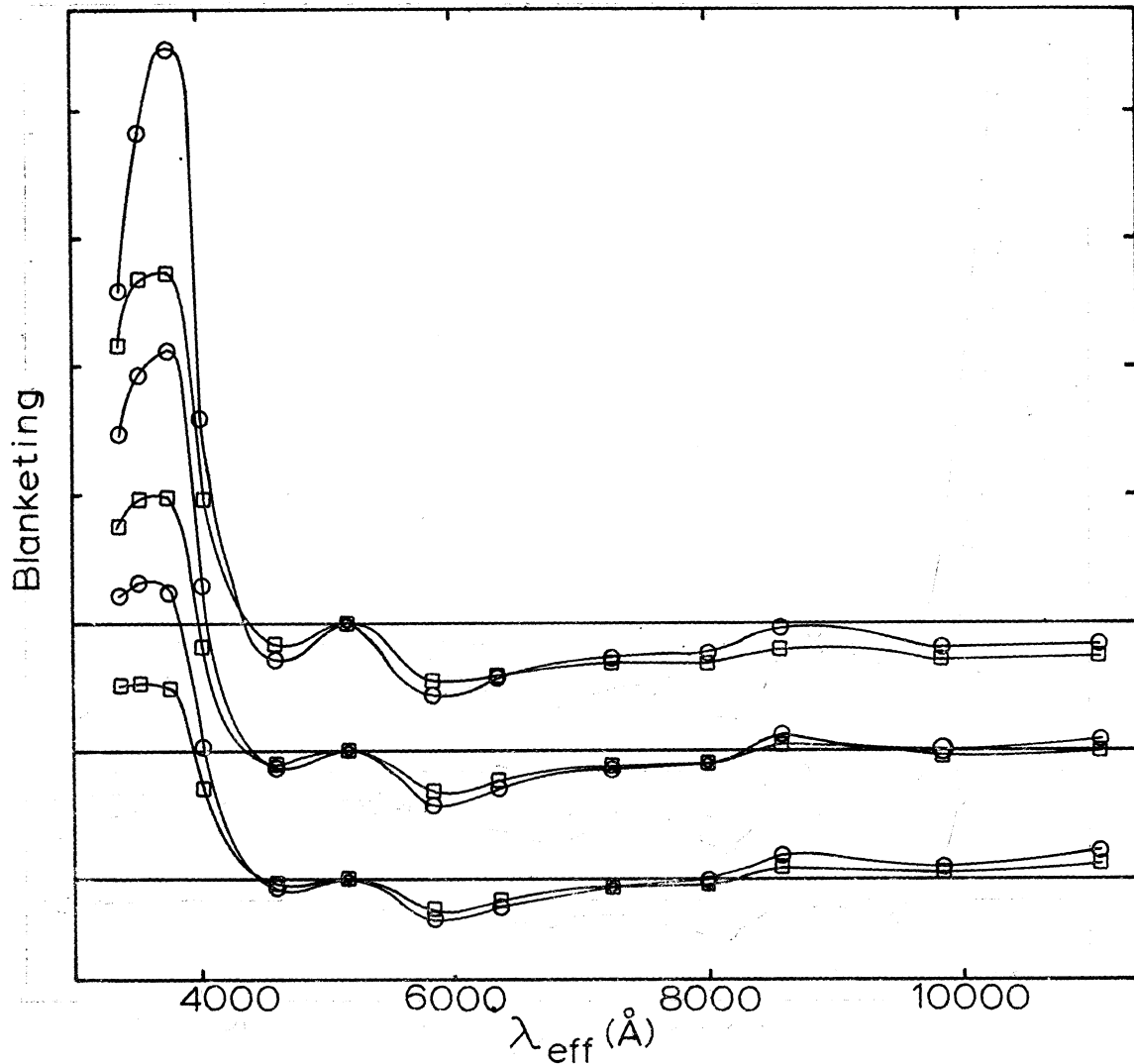
Fig. 8. Theoretical blanketing curves. Squares are for 0.1 solar abundance and circles 0.01. The lower two curves show the blanketing effect at Te = 6500°, the middle two curves at Te = 6000°, and the upper two curves at TE = 5500°. For all curves log g = 4.5. The shift of the horizontal lines and the scale of the ordinate axis are both 0.1 magnitude.

these are obtained by subtracting the $0.1\times$ and $0.01\times$ colors from the $1\times$ colors at constant Te and constant log g. These theoretical curves show only effects of composition.

From Figures 5 to 8 we can draw the following conclusions: (a) The shapes of the blanketing curves remain remarkably similar over the range of Te's and compositions represented by the seven groups implying that a single 13-color metallicity index will be sufficient over the full temperature range

of the subdwarfs. (b) As suggested by Johnson and Mitchell (1968) the $37 - 45$ index seems to be excellent for measuring metallicity since it contains nearly the full sensitivity to composition changes. Other indices such as $35 - 58$ or $37 - 58$ have slightly greater sensitivities but have other disadvantages, such as sensitivity to surface gravity or larger accidental errors of observation. The 37 filter is especially suited for measuring [Fe/H] since it contains within its half-intensity width (Johnson

et al. 1967) a large number of both weak and strong Fe I lines (see Seitter 1970). (c) The filters 45 thru 110 would all be useful for creating temperature-sensitive indices since these have little sensitivity to the overall metallicity effect. Filter 52 is seen to contain somewhat more blanketing than the other filters in this group due to the presence of a number of strong Mg I lines ($\lambda\lambda 5167$, 5173, and 5184). (d) Most stars of Figure 5 also have UBV photometry, and we see that the 37 − 45 versus 45 − 63 diagram has more sensitivity to metallicity than the U − B versus B − V diagram. Stars having a range in δ(U − B) from 0.00 to +0.25 will have approximately a range in δ(37 − 45) of 0.00 to +0.40. (e) The theoretical blanketing curves agree very well with the observational ones except for the 33 and 35 filters at the coolest temperatures. A comparison of Figure 8 with the blanketing curves of groups 2 and 5 shows this clearly. Also, the 33 − 52 and 35 − 52 colors of the (5770, 4.44, 1×, 2) model, which supposedly represents the Sun, show a similar discrepancy from the derived 13-color solar photometry of Mitchell (1975; also Schuster 1976a). These differences probably result from the factors discussed by Relyea and Kurucz (1976).

VI. GRAVITY-DIFFERENCE CURVES

In Figures 9 and 10 are plotted observational gravity-difference curves and in Figure 11 theoretical curves. The observational curves have been obtained in the same manner as the blanketing curves except that giant or subgiant stars, not subdwarfs, have been compared to the Hyades main sequence at constant Te, and 45 − 63 has been corrected for gravity differences using the models. The 13-color photometry of the giants and subgiants comes from Johnson and Mitchell (1975) and from Table 2. The surface gravities need for interpolating the corrections have been estimated from Allen (1973); this rather crude method should not lead to any significant errors since the 45 − 63 gravity corrections are all small (<0.03 magnitude). At Te = 5500° the correction is zero, and so for all stars with Te < 5500° no gravity correction has been applied. Since the 45 − 63 corrections are small and change slowly with temperature, this approxi-

mation should not lead to any problems as long as molecular absorptions do not enter into the 45 − 63 index. For the theoretical curves the log g = 4.5 models are compared to the log g = 3.0 ones at constant Te and constant composition.

By comparing the curves of Figures 9 thru 11 we can conclude the following: (a) The important thing to note is the behavior of filters 33, 35 and 37. Decreasing the surface gravity always makes filters 33 and 35 fainter with respect to filter 37. These filters span the Balmer discontinuity which is sensitive to surface gravity for F stars. However, this behavior of filters 33 and 35 with respect to 37 appears in all of the figures and so must hold over an even wider temperature range—at least from the Te of F0III stars to the Te of K0III. (b) The observational gravity-difference curves show primarily surface gravity differences, but blanketing effects are also present. This clearly demonstrated in the lower part of Figure 10 where two field giants (both G9III) and two Hyades giants (G9III and K0III) have been compared to the Hyades main sequence. The field giants clearly show excess with respect to the Hyades giants for filters 33, 35, 37 and 40. In Figure 12 we have constructed an observational blanketing curve for cool giants by subtracting the average colors of BS6075 and BS6703 from the average colors of the Hyades giants, H28 and H71. This represents a comparison at nearly identical (45 − 63)'s, hence nearly identical Te's. We note that the blanketing curve of Figure 12 is fairly similar in shape to the subdwarf blanketing. (c) A comparison of the theoretical and observational curves shows no significant discrepancies. (d) There are several indices which may be gravity sensitive depending on the temperature range. A good compromise seems to be the index (35 − 52) − (37 − 45) which has several advantages. First, it retains its luminosity sensitivity over a wider temperature range than a simple two filter index; (35 − 52) is sensitive for the hotter stars while (37 − 45) is not, but for cooler stars (35 − 52) is less sensitive and (37 − 45) starts becoming sensitive. Second, the blanketing of this index is nearly zero since the blanketing of (35 − 52) nearly cancels that of (37 − 45); this remains true over a fairly wide temperature range as shown by the unchanging shapes of the blanketing curves. Third, in a (35 − 52) − (37 − 45) versus 45 − 63
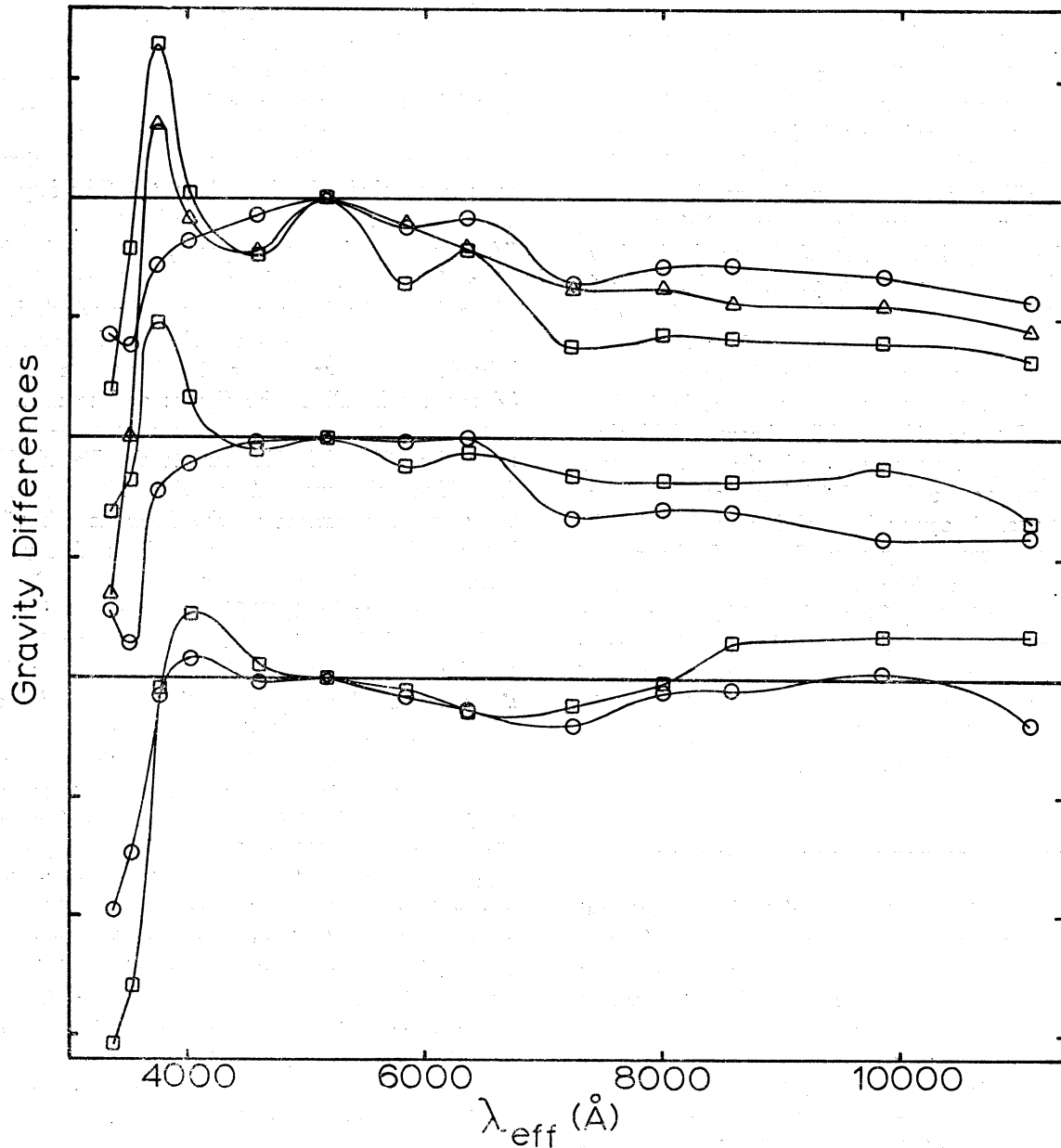
Fig. 9. Observational gravity-difference curves. In the lower part of the figure are plotted two F giants; squares represent BS4031 (F0III, $45 - 63 = 0.453$) and circles BS2930 (F3III, 0.567). In the middle part of the figure circles represent BS5235 (G0IV, 0.764) and squares BS8905 (F8IV, 0.789). At the top circles are plotted for BS6623 (G5IV, 0.919), triangles for BS2803 (F8II, 0.976) and squares for BS7479 (G0II, 0.997). The scale of the ordinate axis is 0.1 magnitude.

diagram lines of constant luminosity are nearly horizontal. (See Figure 13). Hence to determine a star's luminosity class it is not important to measure very accurately its temperature, which compensates

in part for the larger accidental errors of the four-color $(35 - 52) - (37 - 45)$ index. In the following sections the index $(35 - 52) - (37 - 45)$ will be designated by the letter 'G'.
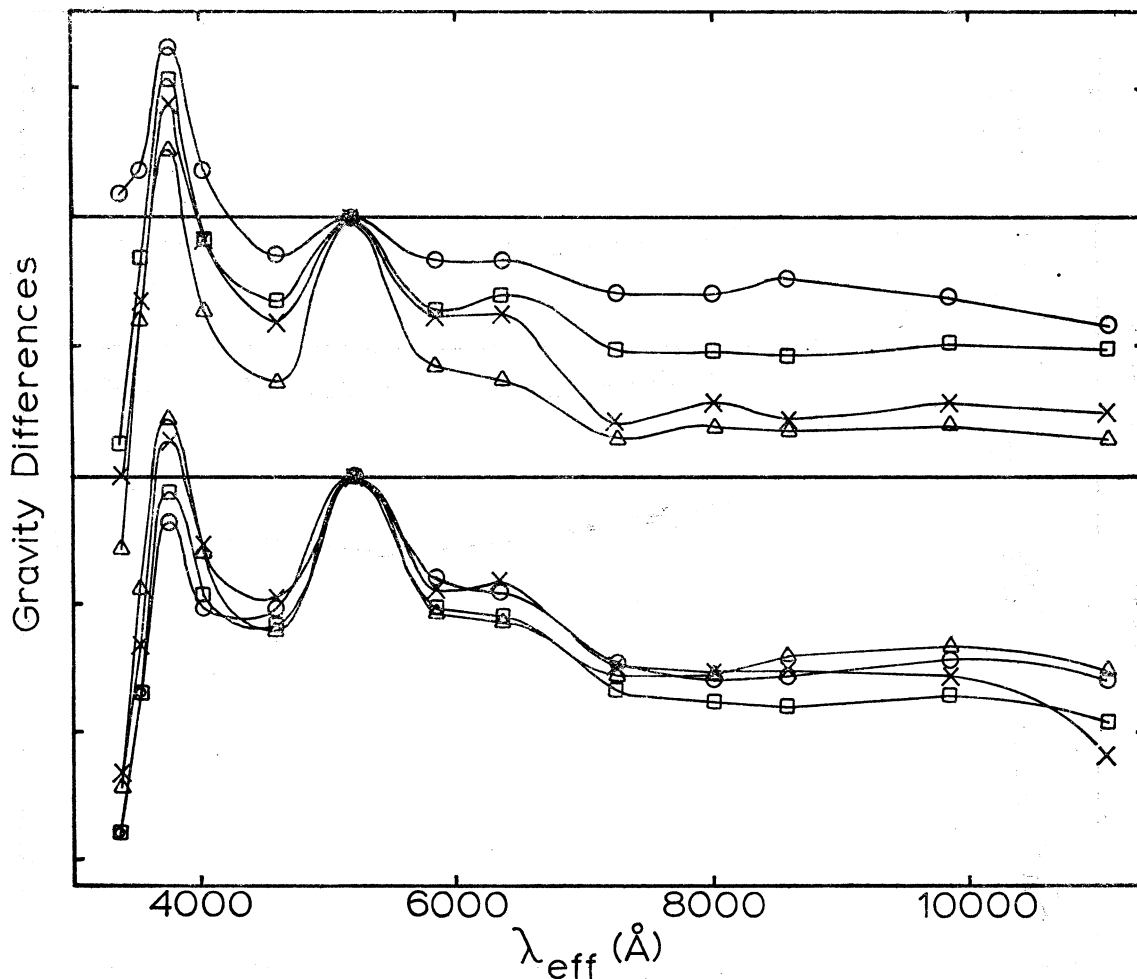
FIG. 10. Observational gravity-difference curves for G giants. In the lower part of the figure circles represent the Hyades giant, H71 (G9III, *45 — 63* = 1.166), squares the Hyades giant, H28 (K0III, 1.196), triangles BS6075 (G9III, 1.194, and X's BS6703 (G9III, 1.155), In the upper part circles represent BS5409 (G2III, 0.900), squares BS1829 (G5III, 1.022), triangles BS442 (G8III, 1.1220), and X's BS5997 (gG2, 1.050). The scale of the ordinate axis is 0.1 magnitude.

VII. THE G VERSUS 45 — 63 DIAGRAM

The preceding analyses have shown that in the range $0.6 < 45 - 63 < 0.95$ the *37 — 45* versus *45 — 63* diagram represents closely a one-to-one transformation of the composition-temperature plane, with little contamination by surface gravity effects. Also, we have seen that in the range of F and G dwarfs and giants the G versus *45 — 63* diagram should correspond closely to the gravity-temperature plane, being nearly independent of blanketing effects. Hence these two diagrams provide very powerful tools for studying metallicity and evolutionary effects in late-F and G stars. Specifically we can use the G versus *45 — 63* diagram to study the degree-of-evolution versus effective temperature status of the extreme subdwarfs and then compare our results with those of Sears and Whitford (1969), Cayrel (1968) and Eggen (1973), who worked in the absolute bolometric magnitude versus effective temperature plane (or equivalent absolute magnitude, infrared color plane).

In Figure 13 we have plotted a G versus *45 — 63* diagram including the Hyades mean colors from Table 5 and subgiants and giants from the work of Johnson and Mitchell (1975) and Schuster
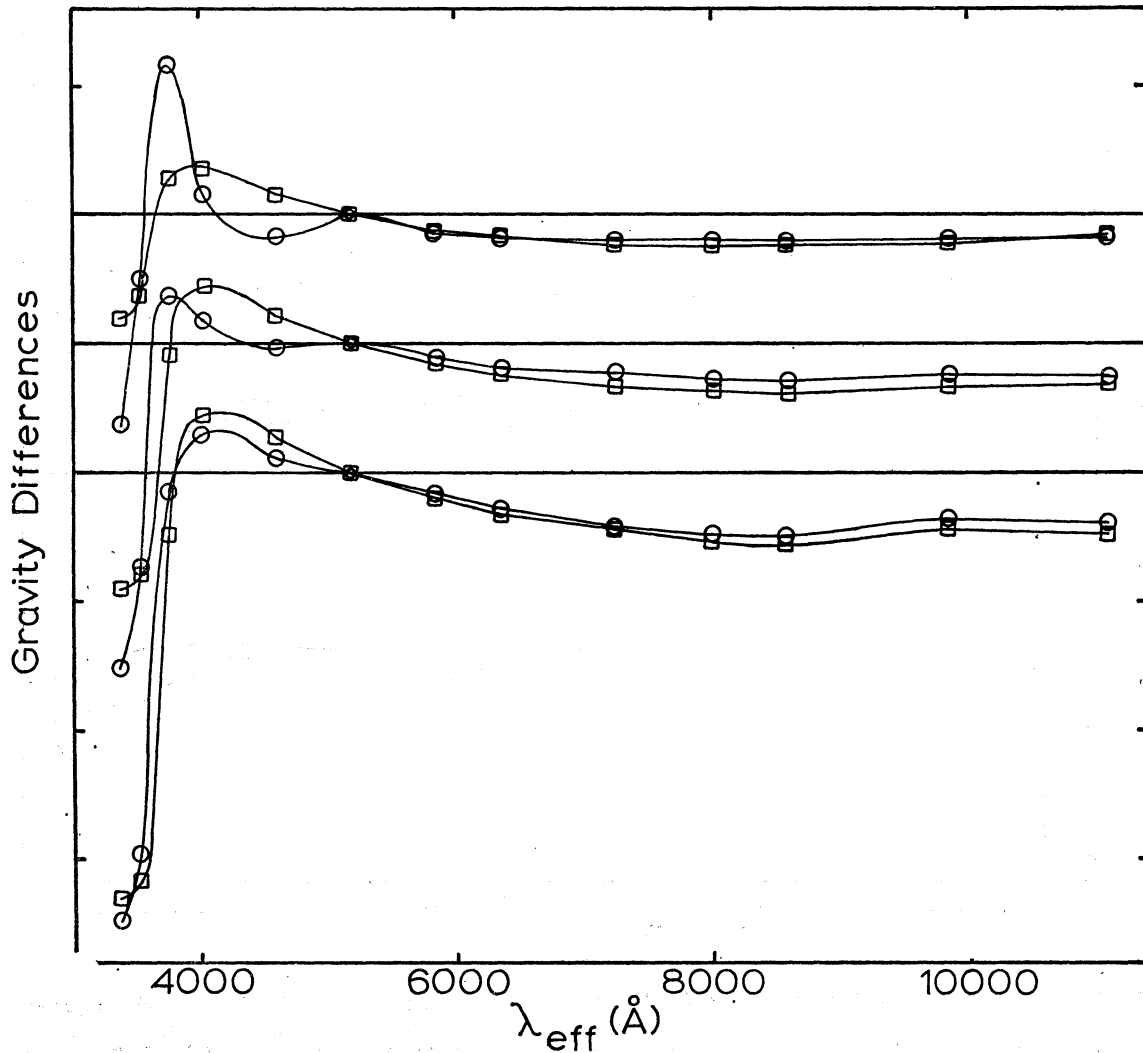
Fig. 11. Theoretical gravity-difference curves. Circles are for solar abundance and squares 0.01 solar abundance. The lower two curves show the effect of gravity at Te = 6500°, the middle two curves Te = 6000°, and the upper two curves Te = 5500°. The shift of the horizontal lines and the scale of the ordinate axis are both 0.1 magnitude.

(1976a). This diagram does indeed seem to be very luminosity sensitive. For $45 - 63 <$ + 0.58 and for $45 - 63 >$ + 1.00 there is a good separation between the Hyades main sequence, the subgiants, and the giants. In the range +0.60 < $45 - 63$ < + 1.0 there are on'y two giants but a number of subgiants, and these maintain a good separation from the Hyades. At $45 - 63$ = 0.77 (~G0) there is at least a 0.1 magnitude separation between the Hyades main sequence and the mean subgiant line. It should also be mentioned that most of the F and G field dwarfs (not plotted in Figure 13) lie slightly

above the line defined by the mean Hyades colors. This is not too surprising since the field stars in general belong to an older population with ages similar to the Sun's (4.5 × 10⁹ years) than the Hyades with an age of about 5 × 10⁸ years (Eggen 1974).

Figure 13 has been drawn to calibrate the G versus $45 - 63$ diagram. Lines of constant luminosity classification, according to the MK system, have been sketched. The mean Hyades main sequence colors have been used to define the locus for luminosity class V while field giants and subgiants were used
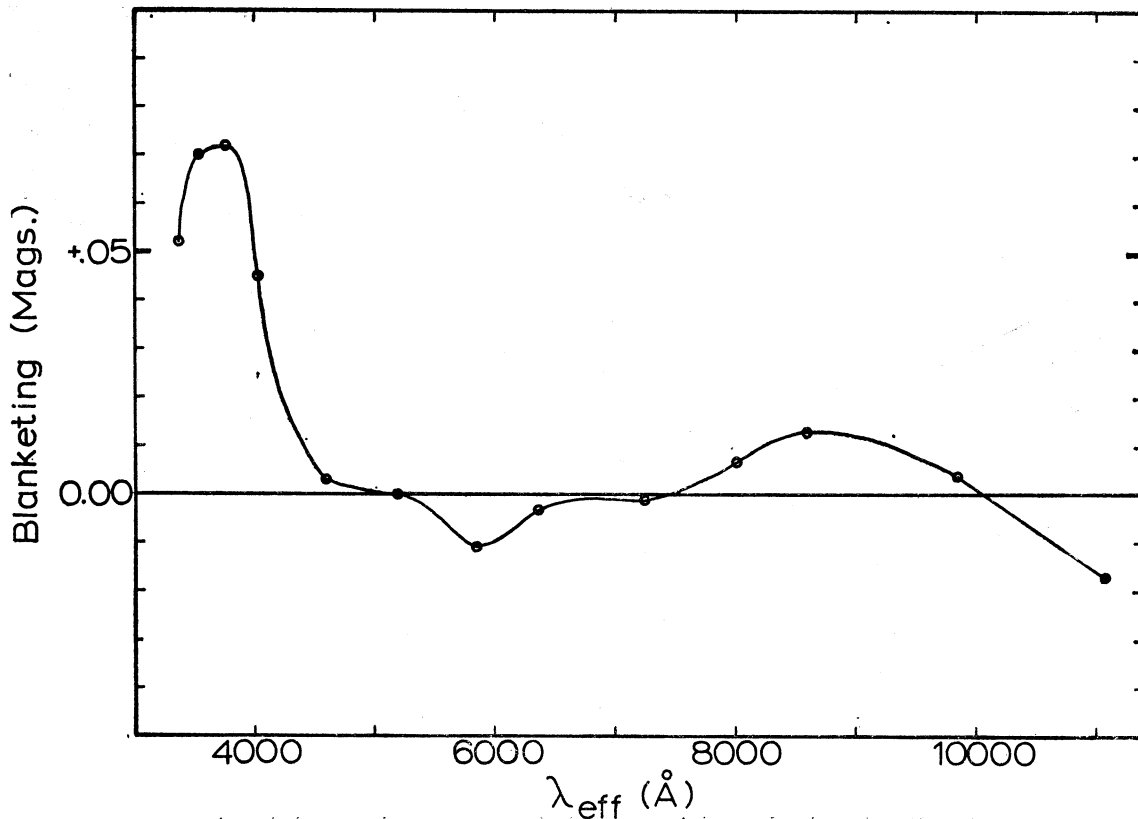
FIG. 12. An observational blanketing curve for cool giants. H28 plus H71 are compared to BS6075 plus BS6703.

for luminosity classes III and IV. For the giants and subgiants only those with 'certain' luminosity classifications, as given by Jaschek *et al.* (1964) and Kennedy and Buscombe (1974), were plotted. By 'certain' we mean that the majority of recent classifications agree as to the luminosity class (but not necessarily the spectral type). Special weight was given to classifications by W. W. Morgan. Also, intermediate types such as IV — V or III — IV were not plotted. For *45 − 63* < 0.60 there are limited observations and so we have used both the observations and the theoretical 13-color photometry for sketching in the lines of constant luminosity class. The solid lines of Figure 13 represent the average main sequence, the average subgiants and the average giants while the dotted lines give the loci that separate the faintest subgiants from the brightest dwarfs (not plotted) and the faintest giants from the brightest subgiants. The separation of types is fairly clear. Out of 124 stars with certain spec-

troscopic luminosity classifications, only eleven have photometric classifications that are different.

In Figure 14 we have replotted the G versus *45 − 63* diagram of Figure 13 but now only the extreme subdwarfs with [Fe/H] < − 1.0 are plotted. The Hyades main sequence line and the subgiant and giant lines have been reproduced exactly as in Figure 13. The dashed lines of Figure 14 mark out five groups of subdwarfs plus an outer envelope for the entire set of subdwarfs (excluding only two 'blue stragglers'). The five numbered regions include nearly the same subdwarfs as regions one to five of Figure 5; the only difference being that G183 − 11D and G206 − 34D have been excluded from group 2 due to the contamination of their photometry. Also plotted at *45 − 63* = 1.270 and G = 0.546 is the red giant HD122563 which has an extreme metal deficiency (Wallerstein *et al.* 1963).

Several interesting points are easily noted in figure 14. First, as discussed by Schuster (1976a), the

258 PHOTOMETRY OF SUBDWARF STARS
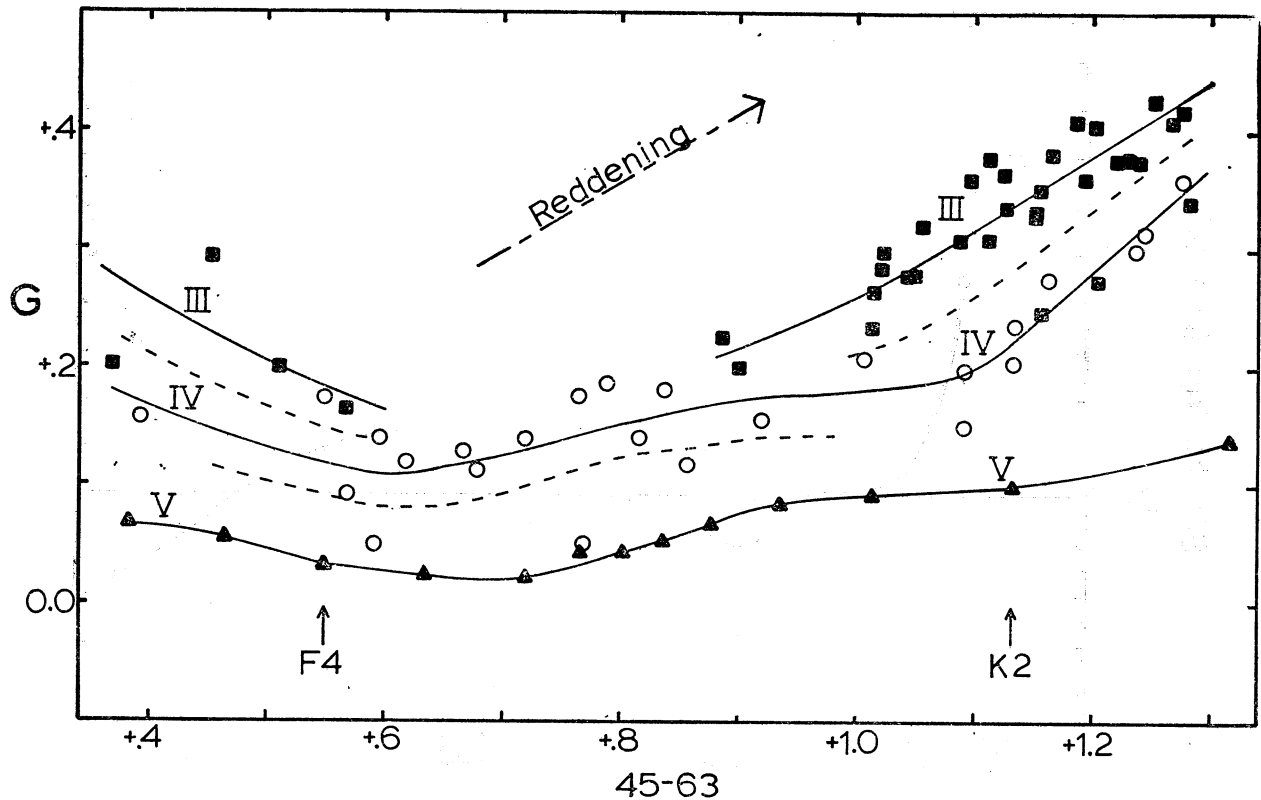
Fig. 13.   G versus *45 − 63*. The triangles and lowest solid line represent the Hyades' main sequence mean colors, the open circles are for subgiants (IV), and the filled squares giants (III).

two stars near the envelope at point 'e' +41°3735 and −9°5491 are obviously not subdwarfs but rather metal-poor giants. These are the 'subdwarfs' marked 'A' and 'B' in Figure 5. Second, one can see that there is a rather sudden cutoff of the subdwarfs at $45 − 63 = 0.59$; only two of the extreme subdwarfs, +25°1981 and −12°2669D, have $45 − 63 < 0.59$. This cutoff is equally apparent using B − V, and Sandage (1964) and Dixon (1963, 1965) have suggested that this cutoff is analogous to the main sequence turnoff of globular clusters; that is subdwarfs which originally had $45 − 63 < 0.59$ have evolved to become metal deficient red giants. Sandage (1964) even went so far as to suggest that the two stars +25°1981 and −12°2669D, which are also bluer than the cutoff in B − V, are equivalent to the blue stragglers seen in some globular clusters (such as M3). Third, remembering that a displacement to more positive G values implies decreasing gravity, we conclude that at least three of the sub-

dwarfs in groups 1 and 2 (−13°482, −17°484, and +44°1910) are in fact metal-poor subgiants which are evolving away from the cutoff. The evolution of these subdwarfs lends support to the idea that the cutoff is analogous to a globular cluster turnoff. And fourth, we note in Figure 14 the surprising fact that there exist a number of subdwarfs redder than the turnoff that appear evolved.

We want to emphasize the analogy between Figure 14 and a globular cluster color-magnitude diagram. Unfortunately no 13-color photometry of individual globular cluster stars exists, and so we must argue by analogy rather than with a direct comparison. The index $45 − 63$ measures primarily the effective temperature and so for a given population type (or metallicity) can be mapped onto B − V. The G index measures primarily the surface gravities of stars while V or Mv gives an indication of the stellar luminosity. We know that at constant Te (and for unique mass-luminosity relations) the
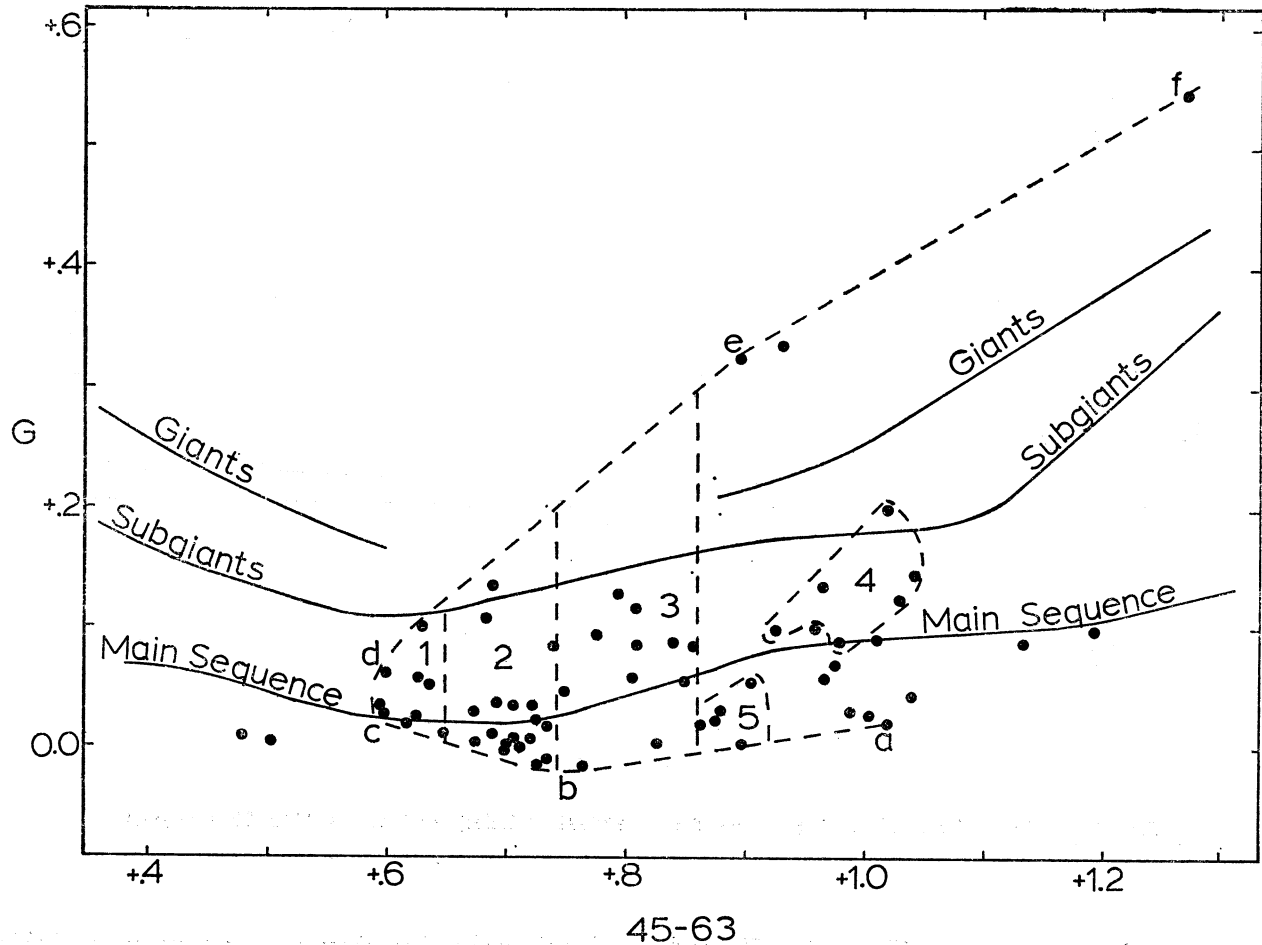
Fig. 14. G versus $45 - 63$ for the extreme metal-poor objects ([Fe/H]$< - 1.0$). The filled circles are for the extreme subdwarfs plus HD122563 (at $45 - 63 = 1.270$ and $G = 0.546$). Other features of this diagram are either the same as in Figure 13 or are explained in the text.

surface gravity is a monotonically decreasing function of the luminosity. Hence, there should be a one-to-one mapping of points in the G versus $45 - 63$ diagram to points in the V versus $B - V$ diagram for extreme Population II objects.

The faintest observed stars in a given globular cluster are the cooler dwarfs ($B - V > 0.6$) which lie along the unevolved Population II main sequence. We claim that the subdwarfs along and slightly above (within $0.06 - 0.07$ magnitude) the line 'ab' of Figure 14, especially those with $45 - 63 > 0.8$, correspond to these unevolved globular cluster stars. As we observe consecutively brighter stars in a globular cluster, we move up the main sequence until we reach a point where the stars begin deviat-

ing from the unevolved sequence. Finally we reach the turnoff where the stars are one to two magnitudes brighter than the unevolved sequence. We argue that the subdwarfs along and slightly above the line 'bc' of Figure 14 correspond to these globular cluster stars which have evolved away from the Population II zero-age line. The part of the envelope 'cd' is the turnoff of our 'globular cluster', and the segment 'def' borders the subgiant-giant branch. If this interpretation is correct, all subdwarfs in groups 1 and 2 are significantly evolved. We propose that for $0.60 < 45 - 63 < 0.75$ the lower envelope of the unevolved Population II sequence in Figure 14 would run parallel to and perhaps $0.04 - 0.08$ magnitude beneath the Hyades main sequence line,
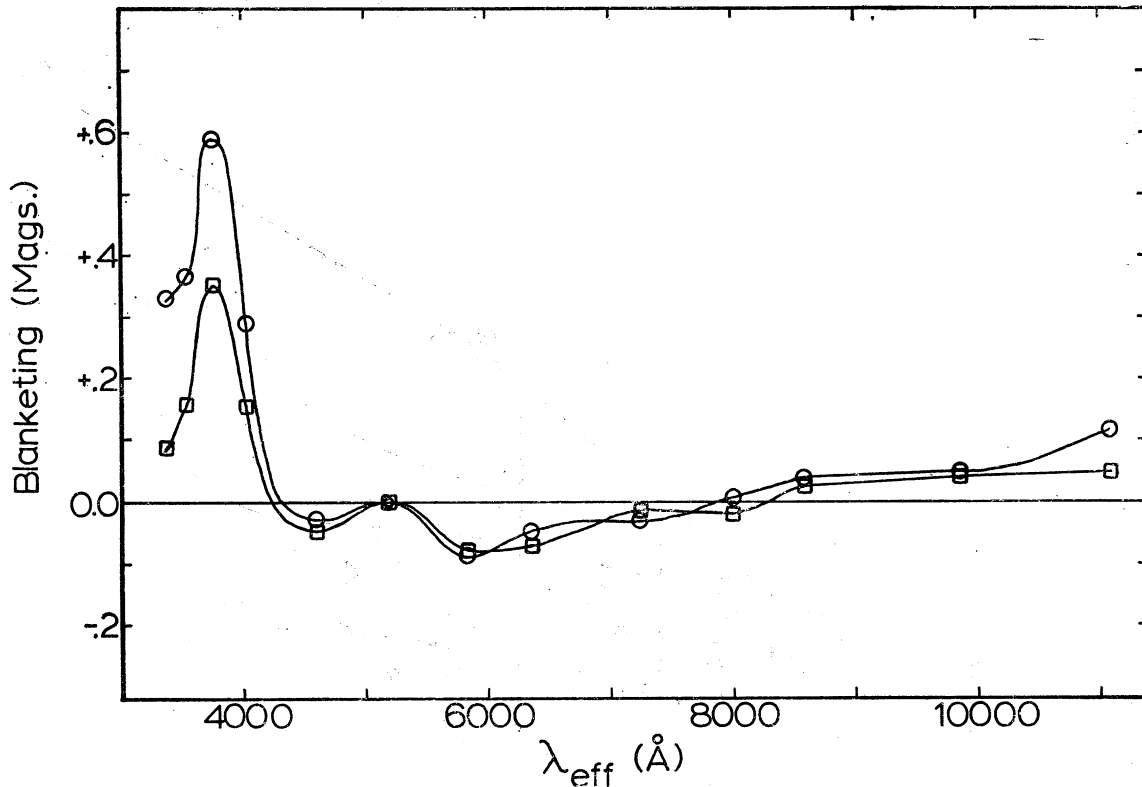
FIG. 15. Observational blanketing curves for — 9°5491 (circles) and for + 41°3735 (squares).

similar to the envelope for *45 − 63* > 0.75, and that just as the cutoff 'cd' implies a rather abrupt cessation in the past of the formation of metal-poor field stars (Dixon 1965, 1966), so does the well defined evolving envelope 'bc'.

The conclusions of Cayrel (1968), Sears and Whitford (1969), and Eggen (1973) agree well with the above results. The (Mbol, Te) diagrams of these investigators show that the hotter subdwarfs are evolved and fall among the disk and Population I dwarfs while the cooler subdwarfs form a sequence distinctly below the disk and Population I sequences. In Figure 14 the subdwarfs near point 'a' have temperatures in the range 5000 − 5200°, the subdwarfs near point 'b' temperatures of 5850 − 6000°, and the turnoff 'cd' corresponds to a temperature of about 6400°. Both Cayrel and Eggen show that for effective temperatures less than about 5500 − 5600° (corresponding to *45 − 63* = 0.85) the separate subdwarf sequence is observed, and so sub-

dwarfs cooler than these temperatures are probably little evolved. This includes most of the subdwarfs in Figure 14 along the line 'ab'. Also, Cayrel concluded that in the (Mbol, Te) diagram the subdwarf sequence crosses the Hyades main sequence due to evolution at Te = 6200°, and he sketched a subdwarf turnoff in the range 6200 − 6300°. The B − V cutoff of Sandage (1964) when corrected to a Hyades composition corresponds also to a turnoff in the temperature range 6200 − 6300° (Johnson 1966). These values agree well with the temperature that we have derived for the turnoff of Figure 14. However, the five stars which define the turnoff of Eggen's (1973, Figure 4) halo sequence have temperatures in the range 5500 − 6000°. In fact, three of these stars are plotted in Figure 14 falling in group 3 and in the redder half of group 2, well to the right of the turnoff. The subdwarf −10°4149 (HD140283) is the most evolved subdwarf in group 3 of Figure 14 and is the second-
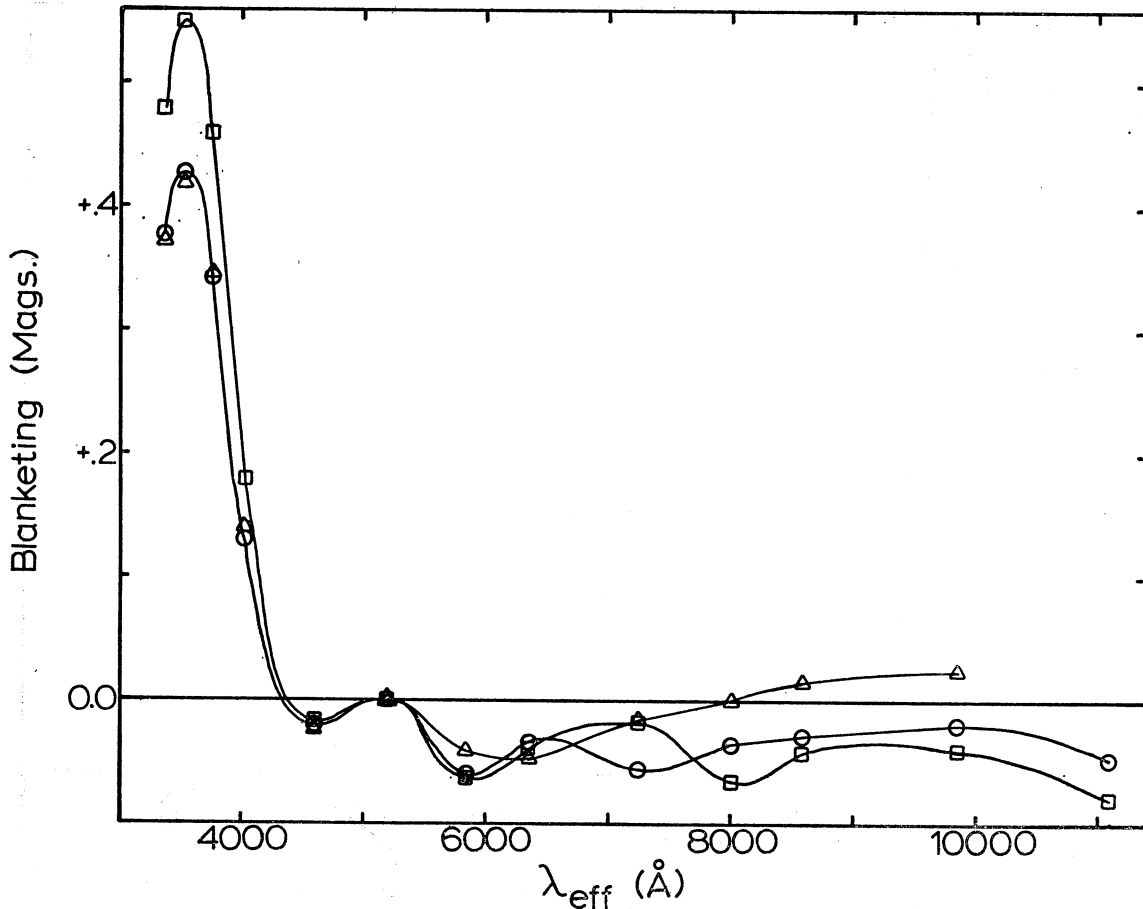
FIG. 16. Observational blanketing curves for BS4550 (circles), for +31°1684 (squares) and for G115-22 (triangles).

most evolved subdwarf in Eggen's halo sequence. We must now return to the problem of the redder subdwarfs in Figure 14 which appear to be evolving.

The turnoff 'cd' of Figure 14 corresponds to a temperature of approximately 6400°, the subdwarfs of group 3 which appear to be evolving fall in the temperature range 5400 — 5850°, and the stars of group 4 have a range of 5000 — 5300°. If we now consult globular cluster isochrones from the metal-deficient stellar models of Demarque (1967), Iben and Faulkner (1968), Rood and Iben (1968), Iben and Rood (1970), and Wagner (1974), we obtain an age in the range (12 — 16) X 10⁹ years for the turnoff, ages of 18 X 10⁹ or greater for the evolving subdwarfs of group 3, and ages greater than 20 X 10⁹ years for group 4. We have taken the helium abundance in the range Y = 0.2 to 0.3 which seems

reasonable considering the discussion of Iben (1974) and the results of Cayrel (1968), Strom and Strom (1967), and Schuster (1976b). According to the ultraviolet excesses, the metal content used has been $Z = 10^{-3}$ to 10^{-4}. There arise two difficulties with these ages. First, the ages of group 4 are uncomfortably large since the most recent determination of the Hubble time (Sandage and Tammann 1975) is in the range (17 — 20) X 10⁹ years. Second, the ages of the subdwarfs in groups 3 and 4 when compared to the turnoff age imply that the subdwarfs were formed over a time interval of at least 2 X 10⁹ years. This contradicts the theory of Eggen, Lynden-Bell and Sandage (1962) which claims that these metal-poor stars formed in only a few times 10⁸ years.
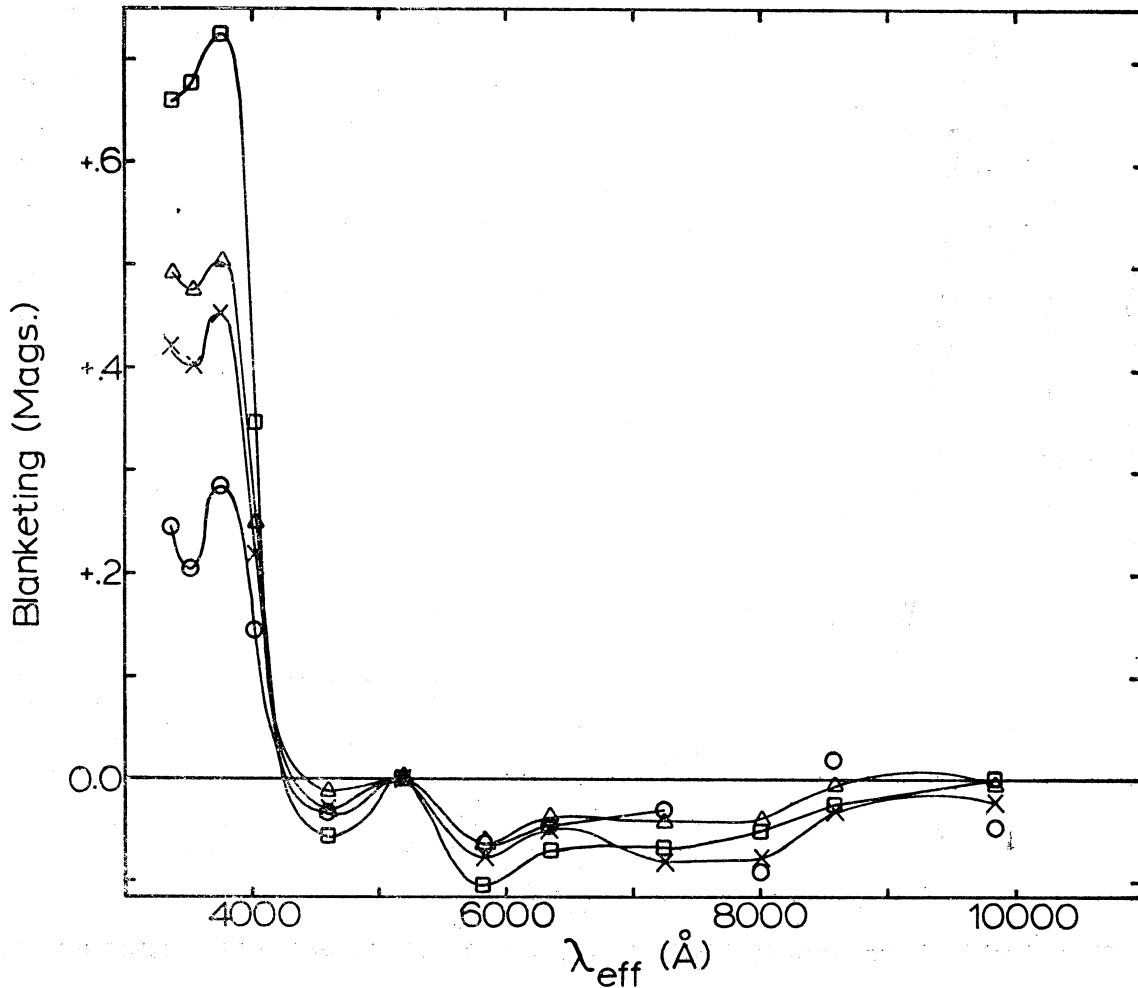
Fig. 17. Observational blanketing curves for $+44°1910$ (circles), for $+13°3683$ (squares), and for $-10°4149$ (crosses). The triangles represent a blanketing curve for $+13°3683$ after dereddening using the interstellar reddening curve of Whitford (1958) and $E(45 - 63) = + 0.18$.

The most logical explanation for the six stars of group 4 is interstellar reddening. In both Figures 5 and 14 the reddening arrows show that these subdwarfs could have intrinsic colors which would place them with the subdwarfs of groups 2 or 3 if the observed colors include a reddening excess of $E(45 - 63) = 0.10 -0.30$. The distribution and distances for four of these subdwarfs are not incompatible with this interpretation. These stars lie within 20° of the galactic plane and have lines of sight passing through, or along the edges of, the reddening clouds sketched by Fitzgerald (1968). The distances for the subdwarfs were obtained using the UBV photom-

etry of Eggen (1964) with the subdwarf sequences of Eggen and Sandage (1962) and using the 13-color photometry with the subdwarf sequence of Schuster (1976b). To explain the colors of these four subdwarfs in Figure 14, we need color excesses only one to three times the values found by Fitzgerald (1968) for the local clouds. This is certainly plausible due to the known patchiness of the interstellar absorption. The other two subdwarfs of group 4 lie more than 40° and more than 85 pcs. from the galactic plane, not in regions studied in detail by Fitzgerald. Figure 5 of Fitzgerald (1968) shows that both of these subdwarfs lie in directions

with $45 - 63$ excesses less than 0.13 at a distance of 500 pcs. These two subdwarfs have distances less than 150 pcs.

However, we cannot readily use this reddening argument to explain the evolved stars of group 3. The two most evolved subdwarfs of group 3, $-10°$ 4149 and $-21°4009$, are within 40 pc. of the Sun and fall in regions of negligible reddening according to Figure 1 of Fitzgerald (1968). Of the eight subdwarfs in group 3 which fall above the Population I main sequence line in Figure 14, only $-21°5703$ and $-13°3834$ are possibly reddened, falling in regions with $45 - 63$ excesses of $0.03 - 0.04$. All eight of these subdwarfs are more than 25° from the galactic plane; four lie somewhat further from the plane than the regions studied in detail by Fitzgerald.

To check whether contamination by a fainter red companion can serve as an explanation for the stars of groups 3 and 4, we have used stars from groups 1, 2, and 3 respectively, to represent the primary components, and several of the redder subdwarfs as the contaminating stars. The absolute 52 magnitudes for the stars were found by fitting them to the subdwarf sequence of Schuster (1976b). We found that in Figure 14 such contamination will shift a star horizontally, making $45-63$ redder but leaving G nearly unchanged. In Figure 5 such contamination mimics approximately interstellar reddening. However, this explanation for the subdwarfs of groups 3 and 4 suffers two serious deficiencies. First, in order to produce the required change in $45 - 63$ requires a contaminating star which is overluminous by 1.0 to 2.5 magnitudes with respect to the subdwarf sequence of the primary. Second, if the contaminating star is not very red, it should be observable either visually or spectroscopically. If the contaminating star is very red, it can be two or more visual magnitudes fainter than the primary and still cause the required change in $45 - 63$, but in this case the resulting blanketing curve for the contaminated photometry would show a sizable infrared excess, specifically in filters 80, 86, and 99. Such an excess is not observed for the stars of groups 3 and 4; for example, see Figure 6. Contamination cannot be used to explain the subdwarfs of groups 3 and 4.

To check for a residual blanketing in the G index we have plotted (not shown) δG versus $\delta(37 - 45)$

for all of the subdwarfs in the range $0.74 < 45 - 63 < 0.86$, including those of group 3, and for all of the subdwarfs in the color range of group 4, $0.92 < 45 - 63 < 1.04$. The ultraviolet excess, $\delta(37 - 45)$, will give a good measure of the total blanketing, and the parameter δG is defined as the difference between a star's G value and the Hyades' main sequence value at constant $45 - 63$. For subdwarfs with $0.74 < 45 - 63 < 0.86$ our plot shows no significant correlation between δG and $\delta(37 - 45)$. Also, any blanketing correction for G would not just apply for $0.74 < 45 - 63 < 0.86$ but for the subdwarfs in the adjacent groups 2 and 5 as well. Hence the lower envelope 'abc' of Figure 14 would also be moved by any blanketing correction, and the subdwarfs of group 3 would continue to apper evolved with respect to this lower envelope.

For subdwarfs with 45-63's similar to group 4 the interpretation is not so straightforward. Excluding the stars of group 4 there appears to be little correlation between δG and $\delta(37$-$45)$. Eleven stars with $[Fe/H] > - 1.0$ have the average values $\delta(37$-$45) = + 0.202$ and $\delta G = - 0.022$, and 8 subdwarfs with $[Fe/H] < - 1.0$ but not in group 4 have $\delta(37$-$45) = + 0.358$ and $\delta G = - 0.035$. Perhaps δG changes by approximately -0.001 due to blanketing for each change of $+0.01$ in $\delta(37$-$45)$. However the six stars of group 4 have the averages $\delta(37$-$45) = + 0.643$ and $\delta G = + 0.042$. These values suggest that the G index has little residual blanketing in this temperature range as shown by the 19 stars not in group 4, and that the δG and $\delta(37$-$45)$ values of group 4 are affected by something else, such as interstellar reddening. In Figures 5 and 14 the reddening lines show that both δG and $\delta(37$-$45)$ will be increased by interstellar reddening.

One might argue that the evolved stars of group 3 in Figure 14 have evolved from the turnoff at 'cd'. We discredit this possibility as follows. The two most evolved subdwarfs of group 2, $-17°484$ and $+44°1910$, and the two most evolved subdwarfs of group 3, $-10°4149$ and $-21°4009$, have been fit to the subgiant branches of M92 and M15 (Sandage 1969), with appropriate corrections for interstellar reddening. The subdwarf B-V values come from Eggen (1964). We find that $-10°4149$ and $-21°4009$ should have an Mv about 0.4 magnitude brighter than $-17°484$ and $+44°1910$ if all four belong to the same metal-poor subgiant sequence. Next, using

this Mv difference, bolometric corrections from Johnson (1966), and the subdwarfs' effective temperatures we calculate that the log g's of $-10°4149$ and $-21°4009$ should be about 0.32 smaller than those of $-17°484$ and $+44°1910$. Also, the data contained in Allen (1973) indicates that the surface gravity along the subgiant line of Figure 14 is nearly constant for $0.65 < 45-63 < 0.85$, and the theoretical 13-color photometry shows that the metal-poor, constant gravity lines have slopes similar to, or greater than, this subgiant line. Finally, the theoretical photometry shows that at G2 ($45-63 = 0.80$) a change of -0.50 for log g gives a change of $+0.05$ to $+0.07$ in the G index. Combining these results we conclude that when $-17°484$ and $+44°1910$ have evolved along their appropriate subgiant sequence to a $45 - 63$ of approximately 0.80, they should be at least 0.03 to 0.05 magnitude above the subgiant line of Figure 14 with G values of $+0.18$ to $+0.20$. In contrast $-10°4149$ and $-21°4009$ have G values of $+0.128$ and $+0.116$. These results suggest that $-17°484$ and $+44°1910$ will evolve along a line in Figure 14 slightly below the dotted envelope 'de' and that $-10°4149$ and $-21°4009$ belong to an evolving sequence different from that of the subdwarfs leaving the turnoff at 'cd'.

Other investigators have encountered similar problems interpreting $-10°4149$ (HD140283). Cayrel (1968) noted that in the Mbol, Te diagram HD140283 is about 500 degrees cooler than the turnoff of an evolution sequence which he sketched for extreme subdwarfs. However, the parallax of HD140283 places it well above his subdwarf sequence and yet not so far above as to fall on the appropriate metal-poor subgiant sequence, quite analogous to the problem found in Figure 14. Strom, Cohen and Strom (1967) found that in order to fit HD140283 (and other similar subdwarfs such as HD19445) in the luminosity, effective temperature plane with the evolutionary tracks of Faulkner and Iben (1966) and with an age less than 20×10^9 years, would require Te's and helium abundances inconsistent with other findings; in any case a single-aged evolutionary track could not fit well all seven subdwarfs analyzed. Cohen and Strom (1968), using model atmospheres, spectrum scans, and high-dispersion spectroscopic data, obtained log g = 3.3 for HD140283 and they note that "this seems a rather low value of surface gravity for a G subdwarf."

Finally, as mentioned above, Eggen (1973) used the subdwarfs HD140283, HD106038, HD108177, HD63077, and $+72°94$ to construct the turnoff of his halo sequence. Yet HD106038 and HD108177 are found in Figure 14 in the redder half of group 2 with $45 - 63 = 0.722$ and 0.698 respectively. We estimated HD63077 to have [Fe/H] = $- 0.67$, and so it is not plotted in Figure 14, but it would fall in group 3 with $45 - 63 = 0.779$. HD140283 is the most evolved subdwarf of group 3, and $+72°94$ was not observed with the 13-color photometers. The B $-$ V's of these 5 subdwarfs range from 0.41 to 0.56 (HD140283 has B $-$ V $= 0.49$) with the average being 0.474. The cutoff in B $-$ V which Sandage (1964) found for stars with $\delta(U - B) >$ 0.16 occurs in the range B $-$ V $= 0.34$ to 0.38 depending on the interstellar reddening correction used.

The above arguments clearly show that the evolving subdwarfs are found over a considerable range of color, B $-$ V or $45 - 63$, and Figure 14 plus the results of Cayrel (1968) and Eggen (1973) indicate that these evolving subdwarfs do not all belong to the same age sequence. This result contradicts some facets of the rapid-galactic-collapse model of Eggen, Lynden-Bell, and Sandage (1962; referred to hereinafter as 'ELS'). Specifically this model predicts that the subdwarfs formed out of gas clouds plummeting toward the galactic center during the stage of galactic collapse and that this galactic collapse took place rapidly in only a few times 10^8 years. ELS argue that the eccentricity of a star's galactic orbit is an adiabatic invariant and so conclude that since the subdwarfs are now observed to have highly eccentric orbits, they must have formed during such a rapid collapse phase. Our resuls indicate a much longer time span for the formation of these metal-poor stars.

We estimate the range of ages in the following manner. The average UBV photometry (Eggen 1964) for the nine stars of group 1 has been compared to the average photometry for the eight most evolved subdwarfs of group 3. Using the blanketing corrections of Wildey, Burbidge, Sandage and Burbidge (1962) and the temperature calibration of Johnson (1966) we obtain an average temperature difference of 430° between the subdwarfs of groups 1 and 3. Using 13-color photometry and Figure 1 we obtain an average temperature difference of 530°.

According to the isochrones of the metal-deficient stellar models of Demarque (1967), Iben and Faulkner (1968), Rood and Iben (1968), Iben and Rood (1970) and Wagner (1974) a temperature range of 400-500° for the turnoff implies an age range of at least 2×10^9 years. The only alternative would be a rather unreasonable range of initial helium abundances with the subdwarfs of group 1 having $Y \sim 0.35$ and those of group 3, $Y \sim 0$.

By comparing globular cluster color-magnitude diagrams to the time-constant loci of metal-deficient stellar models, Rood and Iben (1968) also concluded that for uniform helium abundances an age span of a few times 10^9 years is implied for the extreme Population II objects. As a result Rood and Iben outlined a theory for the early history of the Galaxy which better explains the features of Figure 14 than does the theory of ELS. First, Iben and Rood argued that even if a rapid collapse did occur in the protogalaxy as in the ELS model, matter at the periphery of the halo could not take part. Such stars or gas clouds would need $(0.6 - 1.8) \times 10^9$ years to free fall into the disk or galactic core. Second, they point out that a slow collapse can also produce stars in highly eccentric orbits providing gas pressure is one of the forces maintaining rotational equilibrium. (ELS argued that the gas pressure must be negligible.) Gas clouds which condensed into stars during this slow collapse would have been released from the gas pressure of the protogalaxy and so would have plummeted toward its center in highly eccentric orbits. Finally at some point during the slow collapse the gas density in the protogalaxy reached a high enough value that a burst of star formation occurred leading to a 'fast collapse' in the central regions. At the end of this phase the disk and central core of the galaxy were formed. Since some of the disk material had been previously processed during the slow collapse phase and since processed material continued to fall into the disk from the supernovae, planetary nebulae, and stellar winds of the stars left behind in the halo, the metal abundance of the disk rose very rapidly, in a few times 10^8 years, as in the two-zone galactic model of Ostriker and Thuan (1975). So, very few metal-poor stars were formed in the disk as is observed.

The above model can be used to explain all of the significant features of Figure 14. The turnoff 'cd' of Figure 14 corresponds to the time interval back to the central collapse which formed the Galaxy's disk. After the formation of the disk and its rapid metal enrichment little metal-poor gaseous material remained in the disk or halo to make more recent subdwarfs which would be plotted to the left of the turnoff in Figure 14. The few 'blue stragglers', such as $+25°1981$ and $-12°2669D$, condensed out of the small amount of gaseous material in the outer halo which did not take part in the central collapse and so had a longer interval of time to condense into stars before reaching the metal-enriched disk. The evolved subdwarfs of group 3 formed during the slow collapse phase preceding the central collapse. These subdwarfs of group 3 are actually several times 10^9 years older than those of groups 1 and 2.

However, the subdwarfs' kinematics suggest alternate interpretations for Figure 14 and for the subdwarfs of group 3. Figure 6 of ELS shows h, the angular momentum of a star in its galactic orbit, versus $\delta(U - B)$. The stars in the solar vicinity with $\delta(U - B) > 0.16$ have h values less than about 12×10^2 kpc km/sec. From this data ELS concluded that when the metal-poor stars formed, the Galaxy was not in its present configuration but was collapsing, and they estimate the scale of the collapse. However, ELS plotted the angular momenta ignoring their sign; the h values were plotted as if all the metal-poor stars have the same sense of rotation in their galactic orbits. The Bottlinger diagram of Eggen (Figure 1, 1964) shows that this is not the case; the stars with $\delta(U - B) > 0.16$ are nearly equally divided between those with forward and retrograde orbits. Freeman (1975) points out that catalogs of such stars usually are biased toward objects with low h values since these are most easily found in proper motion surveys, but the existing data suggests that as a group the extreme subdwarfs do not partake in galactic rotation and so have a net angular momentum close to zero. At present the galactic material with zero angular momentum is found in two locations; one, near the galactic nucleus and two, in material falling into the Galaxy from the intergalactic medium.

So, one alternative would be that extreme subdwarfs had their origin in the galactic nucleus. Perhaps during the early history of the Galaxy the nucleus had a phase lasting several times 10^9 years
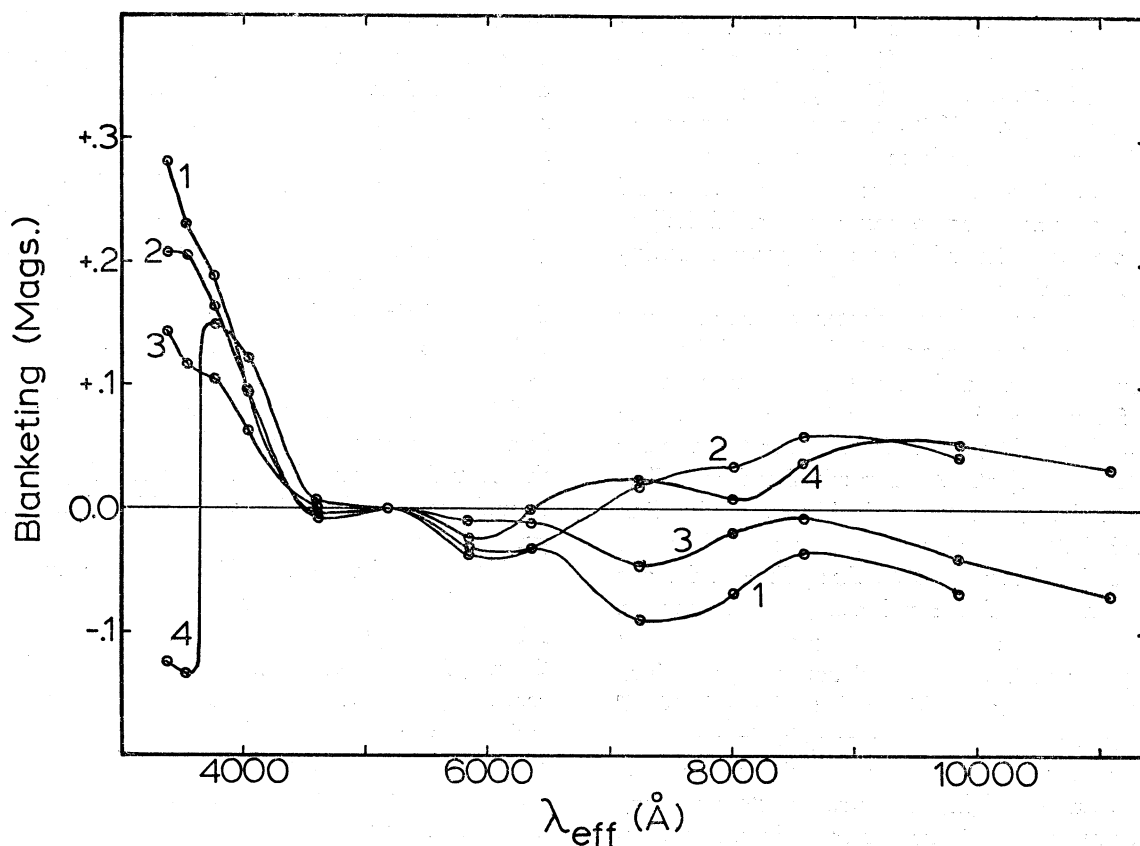
FIG. 18. Observational blanketing curves for four of the hottest metal-poor objects. Curve 1 represents $-12°2669D$, curve 2, $+25°1981$, curve 3, $+30°2536$, and curve 4, $+25°3344$.

when it was very active, ejecting clouds of gas which would later condense into the metal-poor stars. However it is not easy to explain why such an active phase should cease abruptly as required by the turn-off of Figure 14. Also, Freeman (1975) points out that few of the subdwarfs have $|h|$ values small enough to allow penetration to within 1 kpc. of the galactic center, and yet on the average the subdwarfs of group 3 do have smaller perigalactic distances than the other subdwarfs of Figure 14 (Eggen 1964). Of the eight most evolved subdwarfs in group 3, five have perigalactic distances less than 1 kpc.

Another alternative would be that the subdwarfs of group 3 have been captured from the intergalactic material of the Local Group. Gunn (1977) discusses the formation and evolution of massive galactic halos and shows that such halos might form quite naturally from infalling material during the evolution of a galaxy. One of the more likely candidates

for the nature of this infalling material would be low-mass stars formed very early in the universe. However, we would expect that if any such stars are found in the solar vicinity they would exhibit nearly hyperbolic orbits with very large apogalactic distances. The data of Eggen (1964) show that the subdwarfs of group 3 have an average apogalactic distance of about 12 kpc. with the largest distance being 15.4 kpc.

VIII. SOME PARTICULAR BLANKETING CURVES

In Figures 15 thru 18 we give the blanketing curves of some individual stars. These curves reinforce the arguments made in the previous sections and can be used in the interpretation of future 13-color photometry of high velocity and metal-poor F and G-type stars. In Figure 15 we give the 'blan-

keting' curves of $-9°5491$ and $+41°3735$, which are the evolved 'subdwarfs' at point 'e' of Figure 14 and at points 'A' and 'B', respectively, of Figure 5. These curves show a large excess for the $37 - 45$ index and also a large depression of the 33 and 35 filters with respect to the 37 filter. From our previous discussions it is obvious that these stars are metal-poor and highly evolved, Population II red giants. In Figure 16 we give the blanketing curves for three of the subdwarfs, BS4550, $+31°1684$ and G115-22, which fall along the lower envelope 'ab' in Figure 14. For comparison Figure 17 gives the observational blanketing curves for $+44°1910$, $-10°4149$ and $+13°3683$, the most evolved subdwarfs from regions 2, 3 and 4 respectively, of Figure 14. The curve for $+13°3683$ is also given after dereddening using the interstellar reddening curve of Whitford (1958) and assuming $E(45 - 63) = + 0.18$. All of these curves show large $37 - 45$ excesses indicating low metacillity, and the curves of Figure 17 when compared to those of Figure 16 show depressions of the 33 and 35 filters with respect to 37 indicating a much more advanced state of evolution for $+44°1910$, $-10°4149$, and $+13°3683$ than for BS4550, $+31°1684$ and G115-22. As we have argued, $+13°3683$, being in group 4, is probably reddened, and yet even after dereddening its blanketing curve shows evidence of evolution. Probably the intrinsic colors of $+13°3683$ would place it among the evolving subdwarfs of groups 2 or 3.

In Figure 18 are shown the curves for all of the 'subdwarfs' which are bluer than the turnoff at $45 - 63 \sim 0.59$ in Figure 14. There are four such stars — $+25°1981$, $-12°2669D$, $+30°2536$, and $+25°3344$. As mentioned previously the two stars $+25°1981$ and $-12°2669D$ can be considered 'blue stragglers' for the 'globular cluster' of Figure 14 (Sandage 1964). Perhaps $+30°2536$, which has a smaller metal deficiency ($[Fe/H] = - 0.46$), is also in this class. The curve of $-12°2669D$ shows the effects of contamination by a nearby star, and the curve of $+25°1981$ suggests than its surface gravity is larger than that of Hyades dwarfs of equal Te. The star $+25°3344$ (HD161817) has $45 - 63 = 0.293$ and $G = + 0.355$, and its curve shows evidence for a very small surface gravity as well as extreme metal deficiency. This star, which is thought to be a Population II horizontal branch star, has been analyzed spectroscopically by Kodaira (1973)

and by Kodaira, Greenstein and Oke (1969) who found $\log g \sim 2.9$ and $[Fe/H] \sim - 1.6$.

IX. CONCLUSIONS

One of the important results obtained in these analyses is the ability of the 13-color photometry to separate the effects of temperature, metallicity and surface gravity in the energy distributions of F, G and K-type stars. This separation is much better than that obtainable with UBVRI and is as good or better than that of Stromgren four-color.

The temperature indices $45-63$ and $58-99$ have good sensitivities to temperature but small to negligible sensitivities to metallicity and surface gravity. $45 - 63$ covers a part of the spectrum similar to $B - V$, has much smaller blanketing corrections (usually 0.02 magnitude or less), has gravity corrections less than 0.03 magnitude, and for F0 to K2 dwarfs has a greater range than $B - V$ (see Table 5 and Johnson 1966, Table 2). $58 - 99$ covers a part of the spectrum similar to $R - I$, has only slightly larger blanketing corrections (0.04 magnitude or less), has very small gravity corrections (0.01 to 0.02 magnitude), and for F and G-type dwarfs has a much greater range than $R - I$ (see Figure 4). These indices have been theoretically calibrated to give Te in Figures 1 and 2 and will be observationally calibrated after the style of Johnson (1966) and Mendoza (1969) in a following paper.

The composition index $37 - 45$, or its differential $\delta(37 - 45)$, has a very large sensitivity to metallicity effects in the energy distributions of F and G stars. A selection of dwarfs having a range of 0.25 magnitude in $\delta(U - B)$ will have approximately a range of 0.40 in $\delta(37 - 45)$ and approximately 0.15 in Δm_1 (Stromgren 1963). $37 - 45$ is very sensitive to temperature (see Figure 5) thereby increasing somewhat the accidental errors of observation in $\delta(37 - 45)$. However, $\delta(37 - 45)$ itself has only a moderate dependence upon temperature and for the range $0.6 < 45 - 63 < 0.95$ a very small dependence upon gravity; for $45 - 63 > 0.95$ decreasing gravity mimicks decreasing metallicity. In the following paper we will calibrate $\delta(37 - 45)$ in the $(37 - 45, 45 - 63)$ diagram using the $[Fe/H]$ values of Morel et al. (1976).

The G index, $(35 - 52) - (37 - 45)$, is very important for the study of F, G and K-type stars

in that it is sensitive to surface gravity and insensitive to temperature and composition. Whether or not there remain any residual blanketing effects in the G index is open to further study, but our preliminary analyses indicate that such effects must be small.

A second major result of this paper is our ability to draw a clear analogy between the positions of the extreme subdwarfs in the G, $45 - 63$ diagram and globular cluster color-magnitude diagrams. Such comparisons have improved our understanding of the evolutionary status of the subdwarfs and have corroborated the findings of Cayrel (1968), Sears and Whitford (1969), and Eggen (1973), who studied the extreme subdwarfs in the Mbol, Te plane. Since the G, $45 - 63$ diagram does not depend upon stellar parallaxes (as does the Mbol, Te diagram) but depends only upon photometric indices, our result represents a new and completely independent corroboration of these previous works.

In the (G, $45 - 63$) diagram nearly all of the hotter (Te $> 6000°$), extreme subdwarfs are evolved forming a well-defined evolving envelope which terminates in a turnoff at about $45 - 63 = 0.59$. Several of the extreme subdwarfs, $-13°482$, $-17°494$, and $+44°1910$, are evolving from this turnoff and are in fact metal-poor subgiants. A subgiant-giant branch can be sketched for our hypothetical globular cluster using $-9°5491$ and $+41°3735$, which are not subdwarfs but rather metal-poor giants. For $45 - 63 > 0.75$ we argue that in the G, $45 - 63$ diagram the lower envelope of the extreme subdwarfs bounds the unevolved Population II main sequence. A number of the extreme subdwarfs are at least $400°$ cooler than the turnoff of our hypothetical cluster, and yet appear very much evolved from this lower envelope, but not so evolved as to fall near the subgiant-giant branch. The 'evolved' subdwarfs of group 4 are certainly explained by interstellar reddening; evolved subdwarfs at such cool temperatures are not compatible with the age of the universe. However, the evolved subdwarfs of group 3 cannot be explained by reddening, nor by contamination of the photometry, nor by residual blanketing in the G index. These subdwarfs of group 3 really are evolved and at least 2×10^9 years older than the subdwarfs evolving from the turnoff.

So Figure 14 presents us with two important facts concerning the early history of our galaxy.

First, the oldest metal-poorest stars now observed did not all form at once but over a time interval of at least 2×10^9 years. This is shown by the evolving subdwarfs of group 1, 2 and 3. Second, at some point in the past the formation of metal-poor stars stopped rather abruptly, in a few times 10^8 years. The sharp cutoff at $45 - 63 = 0.59$ is evidence for this. The cosmological implications of these two facts are important.

REFERENCES

Allen, C. W. 1973, Astrophysical Quantities, (3rd ed.; London: The Athlone Press), 213.
Borgman, J. 1960, Bull. Astr. Inst. Netherlands, 15, 255.
Borgman, J. 1961, Bull. Astr. Inst. Netherlands, 16, 99.
Borgman, J. 1962, Bull. Astr. Inst. Netherlands, 17, 58.
Cayrel, R. 1968, Ap. J., 151, 997.
Cohen, J. G., and Strom, S. 1968, Ap. J., 151, 623.
Demarque, P. 1967, Ap. J., 149, 117.
Dixon, M. 1963, Observatory, 83, 30.
Dixon, M. 1965, M. N. R. A. S., 129, 51.
Dixon, M. 1966, M. N. R. A. S., 131, 325.
Eggen, O. J. 1963, A. J., 68, 697.
Eggen, O. J. 1964, R. Obs. Bull., No. 84.
Eggen, O. J. 1973, Ap. J., 182, 821.
Eggen, O. J. 1974, Pub. A. S. P., 86, 162.
Eggen, O. J., Lynden-Bell, D., and Sandage, A. R. 1962, Ap J.. 136, 748.
Eggen, O. J., and Sandage, A. R. 1959, M. N. R. A. S., 119, 255.
Eggen, O. J., and Sandage, A. R. 1962, Ap. J., 136, 735.
Faulkner, J., and Iben, I. 1966, Ap. J., 144, 995.
Fitzgerald, M. P. 1968, A. J., 73, 983.
Freeman, K. C. 1975, in Stars and Stellar Systems, Vol. 9, Galaxies and the Universe, eds. A. Sandage, M. Sandage, and J. Kristian (Chicago: The University of Chicago Press), pages 452 and 495.
Gliese, W. 1969, Veröff. Astr. Rechen Inst. Heidelberg, No. 22.
Gunn, J. 1977, Ap. J., 218, 592.
Hoffleit, D. 1964, Catalogue of Bright Stars (New Haven, Conn: Yale University Obs.)
Iben, I., Jr. 1974, Ann. Rev. Astr. and Ap., 12, 215.
Iben, I., Jr., and Faulkner, J. 1968, Ap. J., 153, 101.
Iben, I., Jr., and Rood, R. T. 1970, Ap. J., 159, 605.

Jaschek, C., Conde, H., and Sierra, A. C. 1964, *Catalogue of Stellar Spectra Classified in the Morgan-Keenan System*, (La Plata, Argentina: Observatorio Astronómico).

Johnson, H. L. 1966, *Ann. Rev. Astr. and Ap.*, **4**, 193.

Johnson, H. L., MacArthur, J. W., and Mitchell, R. I. 1968, *Ap. J.*, **152**, 465.

Johnson, H. L., and Mitchell, R. I. 1968, *Ap. J.*, **153**, 213.

Johnson, H. L., and Mitchell, R. I. 1975, *Rev. Mex. Astron. Astrof.*, **1**, 299.

Johnson, H. L., Mitchell, R. I., and Latham, A. S. 1967, *Comm. Lunar and Planet. Lab.*, **6**, 85.

Kennedy, P. M., and Buscombe, W. 1974, *MK Spectral Classifications Published Since Jaschek's La Plata Catalogue* (Evanston, Illinois: Northwestern University Press).

Kodaira, K. 1973, *Astr. and Ap.*, **22**, 273.

Kodaira, K., Greenstein, J. L., and Oke, J. B. 1969, *Ap. J.*, **155**, 525.

Kurucz, R. L. 1970, *Smithsonian Ap. Obs. Spec. Rept.*, No. 309.

Kurucz, R. L. 1974, *Center for Astrophys. Preprint Series*, No. 234.

Kurucks, R. L. 1975, private communicatiion.

Mendoza, E. E. 1969, *Publ. Depto. Astron. Univ. Chile*, **1**, 106.

Mitchell, R. I. 1975, private communication.

Mitchell, R. I., and Johnson, H. L. 1969, *Comm. Lunar and Planet. Lab.*, **8**, 1.

Morel, M., Bentolila, C., Cayrel, G., and Hauck, B. 1976, *Abundance Effects in Classification*, Proc. IAU Symposium No. 72, eds. B. Hauck and P. C. Keenan (Dordrecht: D. Reidel), p. 223.

Morgan, W. W., and Hiltner, W. A. 1965, *Ap. J.*, **141**, 177.

Ostriker, J. P., and Thuan, T. X. 1975, *Ap. J.*, **202**, 353.

Parenago, P. P. 1940, *Astr. J. Soviet Union*, **17**, 1.

Relyea, L. J., and Kurucz, R. L. 1976, *Center for Astrophys. Preprint Series*, No. 600.

Roman, N. G. 1955, *Ap. J. Suppl.*, **2**, 195.

Rood, R., and Iben, I., Jr. 1968, *Ap. J.*, **154**, 215.

Sandage, A. 1964, *Ap. J.*, **139**, 442.

Sandage, A. 1969, *Ap. J.*, **157**, 515.

Sandage, A. R., and Eggen, O. J. 1959, *M. N. R. A. S.*, **119**, 278.

Sandage, A., and Smith, L. L. 1963, *Ap. J.*, **137**, 1057.

Sandage, A., and Tammann, G. A. 1975, *Ap. J.*, **197**, 265.

Schuster, W. J. 1976a, *Rev. Mex. Astron. Astrof.*, **1**, 327.

Schuster, W. J. 1976b, *Ph. D. Dissertation*, University of Arizona, Tucson.

Sears, R. L., and Whitford, A. 1969, *Ap. J.*, **155**, 899.

Seitter, W. C. 1970, *Atlas for Objective Prism Spectra*, Bonner Specktral Atlas I, (Bonn: Ferd. Dummlers Verlag).

Smith, M. 1968, *Pub. A. S. P.*, **80**, 223.

Strom, S., Cohen, J. G., and Strom, K. M. 1967, *Ap. J.*, **147**, 1038.

Strom, S., and Kurucz, R. L. 1966, *J. Quant. Spectrosc. and Rad. Transf.*, **6**, 591.

Strom, S., and Strom, K. M. 1967, *Ap. J.*, **150**, 501.

Strömgren, B. 1963, in *Stars and Stellar Systems*, Vol. 3, *Basic Astronomical Data*, ed. K. Aa. Strand (Chicago: University of Chicago Press), p. 142.

Strömgren, B. 1966, *Ann. Rev. Astr. and Ap.*, **4**, 433.

Wagner, R. L. 1974, *Ap. J.*, **191**, 173.

Wallerstein, G., Greenstein, J. L., Parker, R., Helfer, H. L., and Aller, L. H. 1963, *Ap. J.*, **137**, 280.

Whitford, A. 1958, *A. J.*, **63**, 201.

Wildey, R. L., Burbidge, E. M., Sandage, A. R., and Burbidge, G. R. 1962, *Ap. J.*, **135**, 94.